



Published in final edited form as:

Dev Biol. 2008 February 15; 314(2): 376–392.

Zic1 and Zic4 regulate zebrafish roof plate specification and hindbrain ventricle morphogenesis

Gina E. Elsen¹, Louis Choi², Kathleen Millen³, Yevgenya Grinblat⁴, and Victoria E. Prince^{1,2,5}

¹The Committee on Neurobiology, University of Chicago, 947 East 58th Street, Chicago, IL 60637, USA

²The Committee on Developmental Biology, University of Chicago, 1027 East 57th Street, Chicago, IL 60637, USA

³Department of Human Genetics, University of Chicago, 920 East 58th Street, Chicago, IL 60637, USA

⁴The Department of Zoology and Anatomy, 1117 West Johnson Street, University of Wisconsin, Madison, WI 53706

⁵Department of Organismal Biology and Anatomy, University of Chicago, 1027 East 57th Street, Chicago, IL 60637, USA

Abstract

During development, the lumen of the neural tube develops into a system of brain cavities or ventricles, which play important roles in normal CNS function. We have established that the formation of the hindbrain (4th) ventricle in zebrafish is dependent upon the pleiotropic functions of the genes implicated in human Dandy Walker Malformation, *Zic1* and *Zic4*. Using morpholino knockdown we show that zebrafish *Zic1* and *Zic4* are required for normal morphogenesis of the 4th ventricle. In *Zic1* and/or *Zic4* morphants the ventricle does not open properly, but remains completely or partially fused from the level of rhombomere (r) 2 towards the posterior. In the absence of *Zic* function early hindbrain regionalization and neural crest development remain unaffected, but dorsal hindbrain progenitor cell proliferation is significantly reduced. Importantly, we find that *Zic1* and *Zic4* are required for development of the dorsal roof plate. In *Zic* morphants expression of roof plate markers, including *lmx1b.1* and *lmx1b.2*, is disrupted. We further demonstrate that zebrafish *Lmx1b* function is required for both hindbrain roof plate development and 4th ventricle morphogenesis, confirming that roof plate formation is a critical component of ventricle development. Finally, we show that dorsal rhombomere boundary signaling centers depend on *Zic1* and *Zic4* function and on roof plate signals, and provide evidence that these boundary signals are also required for ventricle morphogenesis. In summary, we conclude that *Zic1* and *Zic4* control zebrafish 4th ventricle morphogenesis by regulating multiple mechanisms including cell proliferation and fate specification in the dorsal hindbrain.

Keywords

Zic genes; zebrafish; hindbrain; ventricle; morphogenesis; proliferation; roof plate; dorsal signaling center; rhombomere boundaries

Corresponding author: Victoria E. Prince Department of Organismal Biology and Anatomy, University of Chicago, 1027 East 57th Street, Chicago, IL 60637, USA Tel. (773) 834-2100 Fax. (773) 702-0037 e-mail. vprince@uchicago.edu.

Publisher's Disclaimer: This is a PDF file of an unedited manuscript that has been accepted for publication. As a service to our customers we are providing this early version of the manuscript. The manuscript will undergo copyediting, typesetting, and review of the resulting proof before it is published in its final citable form. Please note that during the production process errors may be discovered which could affect the content, and all legal disclaimers that apply to the journal pertain.

INTRODUCTION

The ventricles of the brain and the central canal of the spinal cord are connected by a continuous lumen. This ventricular system contains the cerebrospinal fluid (CSF) and serves important functions including control of neural cell proliferation, waste removal and protection against trauma (Miyan et al., 2003; Novak et al., 2000). Although several abnormalities related to brain ventricle size and structure have been described (Bergsneider et al., 2006; McAllister and Chovan, 1998), we lack a detailed understanding of how the ventricular system forms.

Ventricle development is a late stage of the conserved morphogenetic process of neurulation that produces the brain and spinal cord. Neurulation begins as the neural plate transitions into the neural tube; during this process cell movement and rearrangement are coupled with regulated growth and patterning. In zebrafish, neurulation begins around 10 hours post fertilization (hpf), as the left and right sides of the neural plate converge towards the dorsal midline, accompanied by invagination of the neural plate to form the neural keel, a loosely associated solid mass of neural cells without a clearly defined midline (Kimmel et al., 1994; Papan and Campos-Ortega, 1994). This transient stage is followed by the formation of the neural rod at about 17hpf, in which cells become more organized as they start to express junctional complexes (Geldmacher-Voss et al., 2003). In the hindbrain, lumen formation is initiated at 18hpf by generation of an epithelial seam at the midline of the neural rod, followed by a rapid opening of the ventricle as right and left sides of the rod pull apart to produce a hollow neural tube overlain by the dorsal roof plate (Tawk et al., 2007). The transient formation of a neural keel is characteristic of teleost fishes, with amniote neurulation instead proceeding by the uprising of lateral neural folds, which meet at the dorsal midline to form the hollow neural tube (Lowery and Sive, 2004). Despite these species-specific differences, many aspects of zebrafish neurulation are shared with primary neurulation in tetrapod vertebrates. In particular, all vertebrates share an epithelial neural plate and undergo similar cell movements to produce the anterior neural tube (Lowery and Sive, 2004). Formation of the amniote posterior neural tube proceeds through the quite different process of secondary neurulation, in which a mesenchymal cell population cavitates from within (Lowery and Sive, 2004); posterior neurulation has not yet been studied in the zebrafish. Zebrafish neurulation has been best studied in the developing spinal cord (Ciruna et al., 2006; Geldmacher-Voss et al., 2003; Kimmel et al., 1994; Papan and Campos-Ortega, 1994; Schmitz et al., 1993), but more recently has been described in the hindbrain (Hong and Brewster, 2006; Lowery and Sive, 2005; Tawk et al., 2007).

A characteristic of the vertebrate hindbrain is its large, dorsally localized lumen: the 4th ventricle. The 4th ventricle is covered by a roof plate, which is induced from the lateral edges of the neural tube and expands dorsally to form a single-cell layer membrane (Chizhikov and Millen, 2004a; Chizhikov et al., submitted). We do not yet have a good understanding of hindbrain ventricle development, although several zebrafish mutants that disrupt ventricle development have been identified in two large-scale morphology screens (Jiang et al., 1996; Schier et al., 1996). The ventricle phenotypes of three mutants have been characterized in detail. In *parachute/n-cadherin* mutants epithelial integrity is disrupted, leading to impaired early neurulation and hindbrain ventricle morphogenesis defects (Hong and Brewster, 2006; Lele et al., 2002). In *nagie oko/mpp5* mutants the 4th ventricle fails to undergo morphogenesis again due to disruption of epithelial integrity (Lowery and Sive, 2005; Wiелlette et al., 2004). In *snakehead/atp1a1* mutants normal 4th ventricle morphogenesis commences, but the ventricle does not fully inflate due to impaired ion transport (Lowery and Sive, 2005). Lowery and Sive (2005) also reported that blocking cell proliferation leads to reduced opening of the 4th ventricle, but that localized cell death does not contribute to this process.

The embryonic hindbrain is subdivided into 7 segments, termed rhombomeres (r1-r7), which are fated to become the cerebellum, pons, and medulla oblongata (Moens and Prince, 2002). The Hindbrain rhombomeres demonstrate characteristic adhesive/sorting properties, and are separated from each other by morphological boundaries expressing boundary-specific markers (Moens and Prince, 2002). Both rhombomere boundaries and dorsal roof plate of the hindbrain function as sources of secreted signaling molecules, such as Wnts, which help pattern surrounding structures (Amoyel et al., 2005; Chizhikov and Millen, 2005; Riley et al., 2004). Rhombomere boundaries are thought to regulate neurogenesis in adjacent rhombomeres (Trevarrow et al., 1990), while signals from the roof plate regulate cell specification in the dorsal regions of the CNS (Chizhikov and Millen, 2005). Of relevance to hindbrain ventricle development, previous work in zebrafish has shown that disruption of Wnt signaling affects rhombomere boundary patterning in the hindbrain, and this correlates with an inability of the hindbrain to broaden normally (Amoyel et al., 2005). In addition, 4th ventricle development is abnormal in mutant *Dreher/Lmx1a* mice, in which the caudal hindbrain fails to induce the formation of the roof plate (Millonig et al., 2000).

Development of hindbrain structures is disrupted in Dandy Walker Malformation (DWM), a human congenital birth defect characterized by cerebellar malformations and abnormalities of the 4th ventricle. Recently, heterozygous loss of *ZIC1* and *ZIC4* has been shown to underlie DWM (Grinberg et al., 2004). Similarly, genetic analyses have revealed that heterozygous deletion of *Zic1* and *Zic4* in mice causes cerebellar hypoplasia, a phenotype that closely resembles the cerebellar phenotype of DWM patients. Additional human dorsal neural tube abnormalities have been linked to mutations in other *Zic* genes (Grinberg and Millen, 2005). Mutations in the human *Zic2* gene lead to Holoprosencephaly (HPE) (Brown et al., 2001), the most common congenital malformation of the human forebrain associated with midline induction defects and failure to separate the cerebral cortex and other forebrain structures. *Zic2* knockdown in mouse results in failed induction of the roof plate in the forebrain region (Nagai et al., 2000), linking roof plate development with HPE. To date, five *Zic* genes have been described in tetrapods and seven in zebrafish (Keller and Chitnis, 2007; Merzdorf, 2007). These genes encode zinc-finger transcription factors, each containing five zinc-finger domains. During neural development, *Zic* genes are expressed in the dorsal midline of the presumptive CNS in distinct, but overlapping, domains. Functional studies in various vertebrate models have revealed multiple roles for *Zic* family members in CNS development (Aruga, 2004), but the mechanisms by which *Zic* genes exert their effects are largely unknown, with only a limited number of downstream target genes identified (Aruga, 2004; Merzdorf, 2007). In *Xenopus*, gain-of-function studies have suggested that specific *Zic* genes function as neural and/or neural crest inducers (Fujimi et al., 2006; Nakata et al., 2000; Nakata et al., 1998; Brewster et al., 1998). Work in mouse shows that *Zic1* functions to promote neural proliferation and inhibit neuronal differentiation, both in the cerebellum and the dorsal spinal cord (Aruga et al., 2002a; Aruga et al., 2002b). Finally, in zebrafish, the linked genes *zic2* and *zic5* have recently been implicated in regulating growth of the dorsal midbrain (Nyholm et al., 2007). Although zebrafish *zic1* expression has been described (Grinblat et al., 1998), the functions of *zic1* and *zic4* have not been analyzed.

As zebrafish provides an accessible vertebrate model to study the process of ventricle morphogenesis (Lowery and Sive, 2004), we investigate here the roles of zebrafish *Zic1* and *Zic4* in dorsal neural tube development. Similar to mouse (Grinberg and Millen, 2005), we find that zebrafish *zic1* and *zic4* are a linked pair of genes with overlapping dorsal neural tube expression. We provide evidence that zebrafish *Zic1* and *Zic4* function cooperatively to promote 4th ventricle morphogenesis. We find that *Zic1* and *Zic4* regulate cell proliferation in the dorsal hindbrain without affecting early hindbrain regionalization or neural crest development. Moreover, we find that the role of *Zic1* and *Zic4* in ventricle morphogenesis is directly linked to their role in roof plate development. In the absence of *Zic* function,

morphological and molecular markers of roof plate, including expression of *lmx1b.1* and *lmx1b.2* genes, are disrupted. We further demonstrate that zebrafish Lmx1b function is required for hindbrain roof plate development, and that loss of Lmx1b is again sufficient to disrupt 4th ventricle morphogenesis. Finally, we show that Zics regulate the establishment of rhombomere boundary-derived Wnt signals, and that these signals are also necessary for normal ventricle morphogenesis. Taken together, our results suggest that zebrafish Zic1 and Zic4 control hindbrain ventricle formation through their effects on multiple aspects of dorsal hindbrain development. Zic1 and Zic4 regulate proliferation, promote the development of dorsal neural tube derivatives including the roof plate, and link patterning from two hindbrain signaling centers, the roof plate and rhombomere boundaries. Although ventricle morphogenesis of the teleost and amniote hindbrains proceeds through different mechanisms, we suggest that fundamental Zic functions are likely conserved throughout vertebrates, and aspects of zebrafish Zic1 and Zic4 gene function may therefore inform future studies of human Dandy Walker Malformation.

MATERIALS and METHODS

Zebrafish maintenance

Wild-type fish strain *AB were used in this study. Embryos were raised at 28.5°C and stage-matched based on morphological criteria (Kimmel et al., 1995).

Full length Zic4 cloning

Zebrafish *zic4* was identified by analysis of genomic sequence obtained from the *Danio rerio* Sequencing Group at the Sanger Institute (http://www.ensembl.org/Danio_rerio/index.html), based on homology to mouse *Zic4* and proximity to zebrafish *zic1* (Grinblat et al., 1998). To isolate a full-length cDNA clone, a 15-19hpf cDNA library constructed by B. Appel was screened by high-stringency hybridization with a PCR-amplified partial cDNA as probe. (NCBI accession # EF546434).

Antisense morpholino oligonucleotide and mRNA injections

Embryos were microinjected at the one to two-cell stage with 1-15ng morpholino oligonucleotides (MO: GeneTools) dissolved in 1X Danieau's buffer (Nasevicius and Ekker, 2000), or with mRNA as previously described (McClintock et al., 2001). To confirm that microinjections did not cause nonspecific morbidity or morphological defects, control embryos were injected with either 1X Danieau buffer or with an unrelated control morpholino (*hoxc1a* MO: TGATAAGAATTCATGACCGCATCTC). Zic MOs used were:

zic1 MOs

UTR (U): 5'-GTCTCTGCTTACTATTTCTCTGACT-3';

ATG (A): 5'-ACTGTGGTCCTGCGTCCAAGAGCAT-3';

SA: 5'-TTTTACCTAACAAAAACAAAGCAA-3',

zic4 MOs

UTR (U): 5'-GAATAACTTGACAGCAGGCAAATA-3';

ATG (A): 5'-CTTCCCAAAGCATCCACGCTCATTA-3';

SA: 5'-CTTTTCACCTAAAACAACAAAACAG-3'.

A similar range of phenotypes was seen in response to microinjection of each individual Zic MO (Supplemental Table S1). Table S1 summarizes phenotypes obtained in response to injection of individual and co-injected Zic MOs at various concentrations. This initial analysis

was used to establish appropriate injection parameters for further phenotypic analysis (see Table 1). For further analysis we used the concentration of each individual *Zic1* and *Zic4* morpholino that gave the highest percentage of embryos with the phenotype (“dorsal fused” neural tube at the level of the hindbrain, as assessed by *in situ* analysis using *zic1* as a dorsal molecular marker). Other MOs were used as described: *Lmx1b.1* MO and *Lmx1b.2* MO (O’Hara et al., 2005), mismatch *Lmx1b* MO control (O’Hara et al., 2005), *Wnt1* MO (Amoyel et al., 2005), and *Rfng* MO (Cheng et al., 2004).

Whole-mount *in situ* hybridization and Immunohistochemistry

Whole-mount *in situ* hybridization was performed as described (Prince et al., 1998). The *zic4* plasmid was digested with *SacII* and antisense riboprobe synthesized using SP6 RNA polymerase (Promega). Other riboprobes were used as described: *zic1* (Grinblat and Sive, 2001), *zic2a* and *zic5* (Nyholm et al., 2007), *hoxb1a* (McClintock et al., 2001), *ephA4* (Irving et al., 1996), *krox20* (Oxtoby and Jowett, 1993), *pax3* and *pax7* (Seo et al., 1998), *msx-C* (Phillips et al., 2006), *shh* (Krauss et al., 1993), *dlx2a* (Akimenko et al., 1994), *phoxd3* (Stewart et al., 2006), *atoh1.1* and *atoh1.2* (Adolf et al., 2004), *lmx1b.1* (O’Hara et al., 2005) and *lmx1b.2* (gift from Dr. Dae-Gwon Ahn), *gdf6a* (Thisse et al., 2001), *rfng* and *wnt1* (Amoyel et al., 2005). Embryos were scored under the dissecting microscope, before being mounted in glycerol and photographed using a Zeiss Axioskop microscope and Nikon D1 camera. In each experiment injected embryos were subdivided and a portion assayed for neural tube phenotypes, while the remainder of embryos were assayed for changes in gene expression.

TUNEL assay to detect cell death was carried out using the *in situ* Cell Death Detection Kit, AP according to manufacturer’s instructions (Roche). Whole-mount immunohistochemistry was performed as described (McClintock et al., 2001). Primary antibodies used were: anti-HuC/HuD (monoclonal, 1:500, Molecular Probes), anti-phospho Histone3 (pH3, polyclonal, 1:500, Upstate Biotechnology), and anti-BrdU (G3G4, monoclonal, 1:100, Hybridoma Bank). Secondary antibodies were conjugated to Alexa Fluor-488, -546, and -633 (Molecular Probes). Embryos were mounted in glycerol and confocal images acquired using a Zeiss LSM-510 confocal microscope with a X25 objective, and further image processing done with ImageJ. Transverse sections were obtained by embedding stained embryos in Durcupan/Araldite and sectioning at 5µm intervals. In addition, sections of about 50µm were cut manually with micro-scissors.

BrdU treatment, Mitotic Index and Cell Counting

Whole mount embryos were treated with 10 mM BrdU (5-Bromo-2’-Deoxyuridine, Sigma) in 15% DMSO and embryo medium essentially as previously described (Shepard et al., 2004). Briefly, embryos were dechorionated and placed in embryo medium on ice for 15 minutes, followed by 20 minutes incubation on ice in BrdU. Embryos were then placed in pre-warmed embryo media for 3 minutes at 28.5°C, followed by fixation in 4% paraformaldehyde (PFA, Sigma) for 2 hours at room temperature and dehydration to 100% methanol at -20°C. Prior to anti-BrdU antibody staining, embryos were rehydrated and treated with proteinase K (10µg/ml, Roche) for 15 minutes, then fixed in 4% PFA for 30 minutes. After rinsing in dH₂O, embryos were treated with 2N HCl (Sigma) for 1 hour at room temperature. Embryos were then processed for BrdU antibody staining as previously reported (McClintock et al., 2001).

Whole-mount embryos labeled with anti-pH3 antibody to detect proliferating cells were counterstained with the nuclear marker Sytox-green (50µM, Molecular Probes). Embryos were mounted in dorsal view and z-sections of the dorsal hindbrains collected at 3µm intervals through a depth of 60µm. Each individual count of proliferating and total cells was made from three consecutive 3µm sections using ImageJ software as previously described (Lyons et al., 2003), from an invariant 120µm long region of the brain spanning approximately two

rhombomeres adjacent to the otic vesicle. For each specimen two separate counts were performed, one from a dorsally located region and one from a ventrally located region within the 60 μ m dorsal domain encompassing the depth of the ventricle; counts were performed from both sides of the neural tube. Mitotic index (proliferating cells/total number of cells) was then calculated for each embryo. Between 5 and 18 specimens were assayed for each experimental condition. ANOVA tests for comparison of multiple groups were performed using GraphPad Prism 4.03 software; $P < 0.05$ was considered significant.

RESULTS

Zebrafish *zic1* and *zic4* are linked genes expressed in the dorsal neural tube during neurulation

Zic gene family members are typically found in linked, divergently transcribed gene pairs (Aruga, 2004; Grinberg and Millen, 2005). We have identified zebrafish *zic4*, and found that it is closely linked with *zic1* (Grinblat et al., 1998) on chromosome 24 of the zebrafish genome. Zebrafish *zic1* and *zic4* genes are arranged in a characteristic divergent configuration, with 4.34 Kb of intergenic (IG) DNA separating their transcription start sites (Fig. S1). The IG is likely to contain important regulatory sequences that may control transcription of both *zic1* and *zic4*, as has been shown for the *zic2a/zic5* gene pair (Nyholm et al., 2007). *Zic1* and *Zic4* are similarly linked in the human and mouse genomes.

The expression pattern of zebrafish *zic1* at stages up to 24hpf was previously reported (Grinblat et al., 1998; Grinblat and Sive, 2001; Rohr et al., 1999). We compared the expression patterns of *zic1* and *zic4* from gastrulation through larval stages (72hpf). We found that both genes are expressed during gastrulation in the anterior neuroectoderm (Fig. 1A,B asterisks) and lateral edges of the future neural plate (Fig. 1A,B arrows), with the expression onset for *zic1* gene at mid-gastrulation (75% epiboly) and *zic4* at late-gastrulation (90% epiboly). By 13hpf *zic1* and *zic4* expression extend posteriorly into the hindbrain. Comparison with *krox20*, a marker of r3 and r5, shows that *zic1* expression extends posteriorly as far as r4 at this stage, while *zic4* expression is limited to a more anterior domain (Fig. 1C,D). By mid-somitogenesis, at 16hpf (Fig. 1E,F), *zic1* and *zic4* expression localize to the dorsal neural tube throughout its anteroposterior (AP) extent. Their expression is modulated along the AP axis (Fig. 1E,F). In addition, and as previously reported for *zic1*, expression of both *zic1* and *zic4* is detected in telencephalon, diencephalon, midbrain, and somites (arrows in Fig. 1E,F).

In dorsal view, expression of *zic1* (data not shown) and *zic4* highlight the progression of hindbrain ventricle opening between 18 and 24hpf (Fig. 1G-I): ventricle opening commences at the level of r1 (Fig. 1G) and continues posteriorly (Fig. 1H,I). Sections through r5 of 18hpf (Fig. 1G') and 24hpf (Fig. 1I') embryos indicate that, similar to *zic1* (Fig. 2C'), *zic4* expression is restricted to the dorsal neural tube, surrounding the ventricle, including the roof plate (Fig. 1I'). During later stages of zebrafish development (48-72hpf), *zic1* and *zic4* expression remain restricted to the dorsal neural tube (Fig. 1J-M; data not shown), with expression becoming localized within the dorsolateral extent of the neural tube (Fig. 1K'). At 48hpf *zic1* expression is detected in discrete domains in the dorsal midbrain (Fig. 1J); a similar pattern emerges for *zic4*, but in a more medially restricted domain (Fig. 1K). The overlapping expression patterns of *zic1* and *zic4*, taken together with their linked genomic organization, suggest that they may share common regulatory mechanisms.

Altered hindbrain ventricle morphogenesis in *Zic1* and *Zic4* morphants

We used morpholino (MO) knockdown to investigate the functions of *Zic1* and *Zic4*. For each *Zic* we obtained similar results using any of three different MOs (see Supplemental Table 1, Methods and Table 1), whereas injection of an unrelated control MO had no phenotypic

consequence. In addition, we found that use of a *Zic1* splice acceptor (SA) MO specifically reduced the levels of normally processed *zic1* transcript (data not shown). However, as SA MOs had some additional non-specific toxicity (*e.g.* shortened body axis at 24hpf assessed by bright field imaging) our remaining phenotypic analysis was performed using *Zic1* and *Zic4* 5'UTR and /or ATG MOs (Supplemental Table 1). The surviving morphants were assessed at 24hpf for the “dorsal fused neural tube” phenotype using *zic1* as a dorsal marker.

We found that knockdown of *Zic1* and *Zic4* (together or independently) led to a fused hindbrain ventricle phenotype (Fig. 2, Table 1), whereas forebrain and midbrain morphology remained largely unaffected. This phenotype could be visualized in 24hpf live specimens using bright-field microscopy (Fig. 2A,B), or using molecular markers of the dorsal neural tube, such as *zic1* itself (Fig. 2C-H'). For simplification, we only show *Zic1+4* double morphants, but Table 1 includes analysis of both single and double morphants. Note that below we refer to *Zic1* and *Zic4* double morphants as “*Zic* morphants”, “*Zic*-deficient” or “*Zic*-MO injected” embryos. The most severe knockdown phenotype was characterized by a complete fusion of the dorsal hindbrain between r2 and the spinal cord (Fig. 2D, Table 1), and the least severe phenotype was characterized by either a single fusion point, or an incomplete opening of the ventricle (Fig. 2F, Table 1). We also observed intermediate phenotypes with multiple points of fusion along the AP extent of the hindbrain (Fig. 2E, Table 1). Transverse sections through r5 indicated that the normal dorsal opening of the hindbrain (Fig. 2C') is obstructed in *Zic* morphants (Fig. 2D'). We determined that the dorsal fused phenotype does not merely represent a delay in normal neural tube development (Fig. 2G,G'): phenotypes similar to those assessed at 24hpf were observed in 48hpf *Zic* morphants (Fig. 2H,H').

We compared the phenotypes resulting from injection of *Zic1* or *Zic4* MOs alone, with those resulting from co-injection of half the concentration of each MO together, and found that the double knockdown produced a significantly higher percentage of embryos with the most severe complete fusion phenotype (Table 1). This result suggests that the linked *zic1* and *zic4* genes function in a cooperative manner. We also found that *zic1* expression is unaffected in *Zic4* morphants and conversely, *zic4* expression is unaffected in *Zic1* morphants (data not shown), suggesting that these transcription factors do not cross-regulate one another. In addition, hindbrain expression of other members of the *zic* gene family (*zic2a* and *zic5*) was also unaffected by *Zic1* and/or *Zic4* knockdown (data not shown). As the anterior hindbrain ventricle opens on schedule in all our *Zic* knockdowns we conclude that *Zic1* and *Zic4* are probably not required for initial hindbrain ventricle opening at the level of r1, but that both are required for normal morphogenesis of the remainder of the hindbrain ventricle after 18hpf. We attempted to rescue the fused ventricle phenotype by co-injection of *zic1* mRNA together with *Zic1* MO but were unable to restore normal ventricle morphology. Rather, when injected alone *Zic1* mRNA produced similar ventricle phenotypes to those observed with *Zic1* or *Zic4* MOs (data not shown), suggesting that ventricle morphogenesis is sensitive to both decreased and increased *Zic1* and *Zic4* expression levels. Similar failed attempts to rescue hindbrain morphogenesis phenotypes were reported for *Tcf3b* MO (Dorsky et al., 2003), suggesting that hindbrain morphogenesis requires appropriate expression levels of multiple genes.

***Zic1* and *Zic4* are required for normal dorsal hindbrain cell proliferation**

Previous analysis of mouse dorsal spinal cord indicated that *Zic1* functions to promote the expansion of dorsal hindbrain progenitor cells (Aruga et al., 2002b). We therefore tested whether hindbrain cell proliferation is similarly regulated by zebrafish *Zic1* and *Zic4*. Using the pH3 antibody, which labels proliferating cells, at the onset of ventricle opening (18hpf) we found no change in the mitotic index (proliferating cells/total cells) in dorsal hindbrains of either single or double morphants relative to controls. In contrast, at 24hpf, when the ventricle is fully open, we found a 42% reduction of the mitotic index in *Zic1*-deficient hindbrains, 51%

reduction in *Zic4*-deficient hindbrains, and 56% reduction in double knockdowns (Fig. 3A-B). Qualitative analysis of pH3 labeling showed that proliferation was already slightly reduced in 21hpf *Zic*-deficient hindbrains (data not shown). We also assayed proliferation by using BrdU treatment followed by immunostaining with anti-BrdU antibody, to label cells in S-phase of the cell cycle (Fig. S2). We found that in 18hpf embryos the number of hindbrain cells in S-phase did not differ between control embryos and *Zic1+4* morphants (Fig. S2A,B). However, in agreement with our pH3 analysis, 24hpf *Zic1+4* morphants show a drastic reduction in dorsal hindbrain proliferation compared to control embryos (Fig. S2C,D). Increased cell death does not account for the reduced proliferation, as the number of apoptotic cells was equivalent in the presence or absence of *Zic* function (data not shown). Together, these findings reveal that zebrafish *Zic1* and *Zic4* positively regulate dorsal hindbrain cell proliferation during the process of ventricle opening. As proliferation has previously been shown to influence zebrafish ventricle expansion (Lowery and Sive, 2005), reduction of proliferation in *Zic*-deficient hindbrains may contribute to the fused ventricle phenotype.

Dorsal hindbrain fates are disrupted in *Zic1* and *Zic4*-deficient hindbrains

To further investigate the mechanisms of *Zic* function we tested whether anteroposterior (AP) or dorsoventral (DV) hindbrain fates are altered in *Zic1* and *Zic4*-deficient embryos. We found that markers of AP identity (*hoxb1a*, *krox-20*, and *epha4*) and markers of early DV identity (*msx-C*, *pax3*, *pax7*, and *shh*) had indistinguishable expression patterns in control or *Zic*-MO injected specimens (Fig. 4A-D, data not shown), suggesting that early patterning defects do not underlie later ventricle morphology defects. Since *zic* expression is restricted to the dorsal hindbrain, including the roof plate, we asked whether the acquisition of specific dorsal hindbrain cell fates is affected in *Zic* morphants.

The dorsal neural tube gives rise to three cell fates: neural crest cells, dorsal hindbrain progenitors, and roof plate cells (Chizhikov and Millen, 2004a). Using a series of molecular markers we demonstrated that while neural crest is unaffected (Fig. 4E-H), the dorsal progenitors are reduced and the roof plate disrupted or absent in the hindbrains of *Zic* morphants (Fig. 4I-P, Fig. 5A-J). The expression of neural crest progenitor marker *foxd3* in the neural plate border at 1 hpf was indistinguishable in *Zic* morphants (n=23) and controls (n=26) (Fig. 4E,F). Similarly, neural crest migration, as revealed by *dlx2a* expression at 24hpf, was unchanged (n=28) in comparison to controls (n=24) (Fig. 4G,H).

We used *atoh1.1* as a marker of dorsal neural progenitors (Adolf et al., 2004; Koster and Fraser, 2001). In *Zic* morphants, the induction of *atoh1.1* expression at 1 hpf was unaltered (n=31) compared to controls (n=27) (Fig. 4I,J). However, at 18hpf, the stage when ventricle opening initiates, dorsal *atoh1.1* expression levels began to show a slight reduction in *Zic* morphants (30/47) relative to controls (n=56) (Fig. 4K,L). As hindbrain ventricle expansion continues, from 18-24hpf, both the levels and the distribution of expression of *atoh1.1* were significantly reduced (42/54; Fig. 4N,P) compared to controls (n=43; Fig. 4M,O). In *Zic* morphants, by 24hpf, the expression of *atoh1.1* was also significantly reduced in the most anterior part of r1, the presumptive valvula cerebelli (arrows in Fig. 4M-P). Interestingly, reduced anterior r1 *atoh1.1* expression was also observed in 24hpf *Zic4* morphants (55/71, data not shown) but not in *Zic1* morphants (n= 81), suggesting that *Zic4* selectively regulates the expression of *atoh1.1* in this region. Expression of the related gene *atoh1.2* (Adolf et al., 2004) was similarly reduced in hindbrains of *Zic* double morphants (27/32 embryos, data not shown), and again showed a loss of expression in anterior r1 (23/32, data not shown). The gradual reduction observed in the number of *atoh1.1* positive neural progenitors may be related to the reduced global dorsal hindbrain cell proliferation described above. We suggest that *Zic1* and *Zic4* regulation of the expansion of dorsal hindbrain progenitor domains may contribute to normal hindbrain ventricle morphogenesis.

Roof plate cells generated from the most dorsal neural progenitors form a membranous single-cell layer that covers the dorsal aspect of the expanding hindbrain ventricle (Chizhikov and Millen 2004a; Chizhikov et al., submitted). In this study we define hindbrain “roof plate” as including both the one cell-layer structure that expands over the hindbrain as the ventricle opens, and the adjacent most dorsal bilateral regions that are also positive for roof plate marker gene expression. Our transverse sections through the hindbrains of *Zic* morphants suggested that this structure is reduced or absent (Fig. 2D’). Consistent with this finding, we found that molecular markers of the roof plate display disrupted expression in *Zic* morphants. Hindbrain expression of the LIM-homeobox gene *lmx1b.2* initiates at 12hpf in cells that are converging towards the dorsal midline (O’Hara et al., 2005, data not shown). At 15hpf, *lmx1b.2* is expressed in the hindbrain dorsal midline, and then in the one cell-layer roof plate as it expands over the ventricle from 18hpf onwards (O’Hara et al., 2005; Fig. 5A,C,E,G,G’). We found that the duplicate gene *lmx1b.1* shows a very similar expression profile in the dorsal midline, although expression levels are low in comparison to *lmx1b.2* (data not shown). In *Zic* morphants we found that the dorsal midline expression of *lmx1b.2* was disrupted from its onset in the hindbrain dorsal midline (data not shown), and continued to show disruption at 18hpf (33/45, Fig. 5B,D) and 24hpf (42/67, Fig. 5F,H) compared to controls (n=39, Fig. 5A,C and n=52, Fig. 5E,G). At 24hpf dorsal midline *lmx1b.2* expression was variable in *Zic* morphants: some showed no expression along the entire AP extent of the dorsal hindbrain (18/42, Fig. 5H), while in others the loss was in restricted AP domains (24/42, Fig. 5F white arrow). In contrast, the expression of *lmx1b.2* in other brain regions, such as hindbrain ventral serotonergic neurons (Zhao et al., 2006), remained unaffected in *Zic* morphants (Fig. 5A,B arrowheads). Dorsal midline expression of *lmx1b.1* was similarly reduced in *Zic* morphants at stages between 16 and 24hpf (data not shown). Expression of an additional roof plate marker, *gdf6a* (a TGF-beta class gene) (Fig. 5I’, arrow) was similarly lost or disrupted in *Zic* morphants at 24hpf (37/54; with 19/37 absent and 18/37 reduced expression) compared with controls (n=31) (Fig. 5I,J), while *gdf6a* expression in the dorsal retina remained unaltered. We suggest that the variable disruption of roof plate marker expression reflects the severity of ventricle fusion phenotypes, since absence of roof plate markers tends to correlate with regions where the ventricle remains fused (Fig. 5F).

We also examined whether ectopic *Zic* function is sufficient to induce *lmx1b* gene expression and expand the roof plate. As mentioned earlier, *Zic1* mRNA over-expression produced a similar ventricle phenotype to *Zic1* morpholino injection, a phenotype characterized by reduced or absent roof plate. In our *Zic1* over-expression study we found no change in the expression pattern of *lmx1b* genes in the dorsal hindbrain region adjacent to the missing roof plate membrane, suggesting that *Zic1* is necessary but not sufficient for *lmx1b* gene expression.

Previous studies in mouse and chick spinal cord and mouse hindbrain have demonstrated that *Lmx* gene function is required for roof plate induction and growth (Chizhikov and Millen, 2004b; Chizhikov and Millen, 2004c; Chizhikov et al., submitted). Using morpholino knockdown we found that in zebrafish hindbrain, *lmx1b.2* plays a similar role in roof plate development. *Lmx1b.2* knockdown caused reduction or loss of expression of the hindbrain roof plate marker *gdf6a* (17/24) compared to controls (n=31) (Fig. 5K,L). This was accompanied by fusion of the hindbrain ventricle, closely resembling the *Zic* morphant phenotype (compare Fig. 5M,N with Fig. 2C-F and see Table 1). In contrast, knockdown of *Lmx1b.1* function did not disrupt hindbrain ventricle morphogenesis to the extent of *Lmx1b.2* knockdown (Table 1). However, co-injection of MOs targeted against both *lmx1b.1* and *lmx1b.2* genes enhanced both loss of morphological roof plate (data not shown) and the ventricle phenotype assessed using dorsal molecular markers (Table 1). In addition, we found that partial *Zic* knockdown strongly exacerbated the very mild phenotype caused by injection of a low dose of *Lmx1b.2* MO (Table 1), suggesting that *Zic* and *Lmx* genes may function within the same genetic pathway to control roof plate development and ventricle opening.

Although we found that *Lmx* function is required for normal roof plate development, we did not find alteration in expression of *atoh1.1* and *atoh1.2* in *Lmx* morphants (data not shown). Moreover, qualitative analysis of neural proliferation using the pH3 antibody in *Lmx* morphants further indicated that dorsal neural proliferation is unaffected (data not shown), suggesting that the effect of *zic1* and *zic4* genes on dorsal neural progenitors is independent of their role in roof plate development. In summary, our experiments suggest that *Zic1* and *Zic4* are necessary for roof plate development, and that absence of roof plate cells correlates with ventricle fusion.

Zic1 and Zic4 regulate rhombomere boundary-derived Wnt signals

Previous studies have suggested that zebrafish rhombomere boundaries are sources of Wnt signals that function to pattern and control hindbrain neurogenesis (Cheng et al., 2004; Riley et al., 2004; Amoyel et al., 2005). In addition, *wnt1* has been found to play signaling and growth-promoting roles in both the midbrain/hindbrain boundary (Wurst and Bally-Cuif, 2001) and the dorsal neural tube (Megason and McMahon, 2002). Amoyel and colleagues (2005) reported that *wnt1* is expressed at elevated levels in the dorsal part of rhombomere boundaries by 16hpf, as well as at lower levels in dorsal hindbrain, and in the expanded roof plate (by 24hpf), except at the level of r1 where no expression is detected (Amoyel et al., 2005; Fig. 6A,C,E). Thus, in the hindbrain, *wnt1* is expressed within the dorsal *zic1* and *zic4* expression domain over the entire time period of the neurulation process (compare Fig. S4B' with Fig. 2C' and Fig. 1I'). At 16hpf, we found that *wnt1* expression was unaffected in *Zic* morphants (n=23) compared to controls (n=31) (Fig. 6A,B). By contrast, at 19hpf (n=42) and 24hpf (n=49), when ventricle morphogenesis is normally in progress, we found that *wnt1* expression was specifically down-regulated in rhombomere boundaries of *Zic* morphants (25/35 and 45/61 respectively) (Fig. 6C-F). Due to loss of roof plate in *Zic* morphants (discussed earlier), the remaining expression of *wnt1* appeared to be localized to the most dorsal aspect of the hindbrain (Fig. 6D,F). We observed a similar down-regulation of *wnt3a* and *wnt10* expression in rhombomere boundaries at 24hpf (data not shown). Amoyel et al. (2005) reported that loss of *wnt1* from boundaries led to an expansion of the rhombomere boundary marker *rfg*. Consistent with this result, we confirmed that in *Zic* morphants not only was *wnt1* down-regulated in rhombomere boundaries, but there was a concomitant expansion of *rfg* into the rhombomere territory at 19hpf (19/26) and 24hpf (31/44) compared to controls (n=22 and n=39 respectively) (Fig. 6I-L), while expression of *rfg* was unaffected at 16hpf (n=21) compared to controls (n=34) (Fig. 6G,H). As previously reported in *Wnt1* morphants (Amoyel et al., 2005), *rfg* did not expand into the r4 territory of *Zic* morphants (Fig. 6J,L).

As disruption of Wnt signaling at rhombomere boundaries is reported to disrupt neuronal differentiation (Amoyel et al., 2005), we examined hindbrain neuronal differentiation in *Zic* morphants using Hu-antibody, which labels postmitotic neurons in clusters within rhombomeres (Fig. S3). In *Zic* morphants we found that the segment-restricted pattern of neuronal differentiation is disorganized at 24hpf (17/27) compared with controls (n=38), with Hu-positive neurons located not only in the centers of rhombomeres as in normal specimens, but also within rhombomere boundaries (Fig. S3). This disorganized neuronal pattern is consistent with a failure of rhombomere boundaries to properly pattern the position of neurons within adjacent rhombomeres.

To address further whether Wnt signals play a role in ventricle morphogenesis, we knocked-down *Wnt1* (as described in Amoyel et al., 2005) and assessed ventricle development using *zic1* and *zic4* as dorsal markers. We found that *Wnt1* knockdown also caused a ventricle fusion phenotype reminiscent of *Zic* morphant phenotype at 24hpf (40/51) (compare Fig. 6P,V,Q,W with Fig. 2C-F), compared to controls (n=55). As *wnt1* is expressed in the dorsal neural tube and roof plate as well as in rhombomere boundaries, this result did not allow us to distinguish

in which of these regions Wnt1 functions to regulate ventricle morphogenesis. We therefore made use of Rfng knockdown, which has been shown to cause specific loss of *wnt1* expression only in rhombomere boundaries (Amoyel et al., 2005). As expected, in Rfng morphants, *wnt1* expression was downregulated in rhombomere boundary cells (39/43, data not shown). This indirect knockdown of Wnt1 function in boundaries only, again caused ventricle fusions reminiscent of Zic morphant phenotype (31/42) compared with controls (n=36) (compare Fig. 6P,V,R,Y with Fig. 2C-F), suggesting that intact Wnt signals in rhombomere boundaries are necessary for normal hindbrain ventricle morphogenesis. As zebrafish *zic2* and *zic5* genes were previously shown to be positively regulated by Wnt signaling in the midbrain (Nyholm et al., 2007), we asked whether expression of *zic1* and *zic4* in the hindbrain is altered in Wnt1 or Rfng knocked-down embryos. We found no change in *zic1* or *zic4* expression in the hindbrains of Wnt1 and Rfng morphants, either before ventricle opening at 18hpf (Fig. 6M-O), or once the ventricle is open at 24hpf (Fig. 6P-Y). These results suggest that specific members of the zebrafish *zic* gene family are subject to different regulation at particular AP levels of the CNS. In summary, we conclude that Zic1 and Zic4 function in the dorsal hindbrain to positively regulate *wnt* gene expression in dorsal rhombomere boundaries, and that rhombomere boundary-derived Wnt signals are in turn necessary for normal hindbrain ventricle morphogenesis.

Roof-plate dependent regulation of rhombomere boundary signals

Interestingly, simultaneous knockdown of both *lmx1b.1* and *lmx1b.2* roof plate genes (denoted as Lmx1b MO) also led to a selective reduction of *wnt1* expression in rhombomere boundaries at 24hpf (31/59, Fig. 7G,H) compared to controls (n=67, Fig. 7E,F), while no change in *wnt1* expression was observed in rhombomere boundaries before ventricle opening at 18hpf (n=43, Fig. 7C,D) compared to controls (n=37, Fig. 7A,B). By contrast, complete loss of *wnt1* expression at the midbrain-hindbrain boundary (MHB) was observed both at 18hpf and 24hpf in Lmx1b morphants (Fig. 7C,D,G,H, asterisks) compared to controls (Fig. 7A,B,E,F) as previously reported (O'Hara et al., 2005). This reduction of *wnt1* rhombomere boundary expression was again coupled with expansion of *rfng* into rhombomere territories at 24hpf but not at 18hpf (data not shown) as in Zic morphants. As Lmx1b function is necessary for roof plate development we conclude that signals from the roof plate are required for maintenance of the dorsal rhombomere boundary signaling centers.

We also addressed whether Wnts in the dorsal hindbrain region, including the roof plate, might in turn regulate *lmx1b* gene expression. At 24hpf, the expression of *lmx1b.2* is normally restricted to the roof plate region, encompassing the expanded one cell layer membrane across the hindbrain ventricle, as well as bilaterally in the neuroepithelial “shoulder” regions (black arrow in Fig. S4A') directly adjacent to the expanded roof plate (Fig. S4A,A'). Expression of *wnt1* overlaps *lmx1b.2* in the expanded roof plate at 24hpf (black arrow in Fig. S4B'), and is additionally localized to the dorsal half of the hindbrain (Fig. S4B,B'). We found that in Wnt1 morphants *lmx1b.2* expression was expanded in the dorsal hindbrain, both at 18hpf (40/42, Fig. 7K,L) compared to controls (n=49, Fig. 7I,J) and at 24hpf (55/56, Fig. 7Q,R) compared to controls (n=66, Fig. 7O,P). However, when Wnt1 was down-regulated only in rhombomere boundaries, using Rfng morphants, *lmx1b.2* expression was not affected both before ventricle opening at 18hpf (n=35, Fig. 7M,N) and after ventricle opening at 24hpf (n=44, Fig. 7S,T) suggesting that the negative regulation of *lmx1b.2* in the dorsal hindbrain does not depend on signals from rhombomere boundaries. We conclude that Wnt signaling in the dorsal hindbrain functions to restrict *lmx1b.2* expression to the roof plate, including the “shoulder” region.

DISCUSSION

In this study we have investigated the functions of zebrafish *zic1* and *zic4*, two closely linked genes that share very similar patterns of expression in the dorsal neural tube. We have established that zebrafish Zic1 and Zic4 function cooperatively to control hindbrain ventricle morphogenesis. In Zic1 and/or Zic4-deficient specimens the hindbrain ventricle does not expand in the usual manner and instead remains partially or completely fused from the level of r2 towards the posterior. In contrast, development of neural plate and neural keel are independent of these Zics, as are neural crest development and early regional patterning of the hindbrain. Our data are consistent with a model in which disruption of 4th ventricle morphogenesis is a consequence of both disrupted dorsal cell fates and disrupted proliferation in the hindbrain (Fig. 8). Specifically, Zic-deficient hindbrains lack roof plate and dorsal rhombomere boundary-derived Wnt signals, show reduced dorsal neural proliferation, and reduced numbers of dorsal neuronal progenitors. In Zic-deficient embryos roof plate specification is disrupted shortly before the onset of ventricle opening, whereas the effects on proliferation and rhombomere boundaries occur during the initial stages of ventricle formation. We propose that the various functions we have uncovered for the Zic1 and Zic4 transcription factors normally work in rapid temporal sequence to control 4th ventricle morphogenesis.

Zic regulation of neural proliferation impacts hindbrain ventricle opening

Regulation of cell proliferation has generally been considered an important mechanism that controls embryonic morphogenesis. Alterations in cell cycle may modulate the shape of individual cells and cellular movements (Kahane and Kalcheim, 1998), as both elevated and low rates of cell proliferation have been shown to affect tissue morphogenesis (Lowery and Sive, 2005; Song et al., 2004). Early during neurulation, cell division is critical for the initial formation of the neural tube (Ciruna et al., 2006; Concha and Adams, 1998; Geldmacher-Voss et al., 2003; Tawk et al., 2007). Similarly, differential proliferation within the ventricular zone may regulate later stage cell behavior to allow the lumen to open, perhaps by promoting loss of cell-cell interactions at the midline or by providing active forces to drive morphogenetic movements. Consistent with a role for cell proliferation in the process of ventricle morphogenesis, it has been shown that reduction of cell proliferation using DNA replication inhibitors prevents proper hindbrain ventricle expansion (Lowery and Sive, 2005). We have demonstrated that hindbrain dorsal cell proliferation is also downregulated in Zic1 and/or Zic4 morphants after 18hpf (Fig. 3 and Fig. S2). The dorsal proliferative zone is restricted to a defined layer immediately adjacent to the hindbrain ventricle (Lyons et al., 2003); as *zic1* and *zic4* expression surrounds the expanding ventricle, we suggest that one role of these Zics is to positively regulate dorsal hindbrain proliferation and hence to allow ventricular expansion after 18hpf. The reduction in dorsal neural proliferation rates likely also underlies the overall reduction of *atoh1*-expressing neural progenitor cells in the dorsal hindbrain (Fig. 4M,P).

The role we propose for zebrafish Zic1 and Zic4 in maintaining progenitor proliferation is consistent with the functions of Zics in other contexts. In *Zic1*^{-/-} mutant mice, the number of proliferating granule cell precursors is decreased in the external granular layer of the cerebellum, a defect that may underlie severe cerebellar hypoplasia coupled with folial patterning defects (Aruga et al., 1998). Similarly, *Zic4*^{+/-} mice also show cerebellar hypoplasia and mild foliation defects, a phenotype that is exacerbated in *Zic1*^{+/-}; *Zic4*^{+/-} mice (Grinberg et al., 2004). Further, a recent study showed that two other linked *zic* genes in zebrafish, *zic2a* and *zic5*, promote neural proliferation in an adjacent brain subdivision, the midbrain tectum, and that Zic2a+5-deficient embryos exhibit profound midbrain and hindbrain ventricle morphogenesis defects (Nyholm et al., 2007).

Loss of Zic1 and Zic4 function disrupts roof plate development in the hindbrain

As the hindbrain ventricle expands, a dorsal overlying single-cell membrane, the roof plate, forms. This expansion is not uniform along the AP length of the hindbrain, as differential growth at specific levels correlates with the rhomboid shape of the hindbrain. Zic genes are not only expressed in the neuroepithelium surrounding the ventricle but also in roof plate cells. In Zic-deficient zebrafish embryos we found that the fused hindbrain ventricle phenotype correlated with loss or reduction of the roof plate markers *lmx1b1.1*, *lmx1b.2* and *gdf6a*. The zebrafish *gdf6a* (*growth differentiation factor 6a*) gene (Thiese et al., 2001) is a member of the same gene superfamily (TGF-beta) as mouse roof plate marker *Gdf7* (Chizhikov and Millen, 2005), but is not the direct ortholog of this gene (Davidson et al., 1999). We noted that the phenotype caused by knockdown of Zic1 and Zic4 function in zebrafish is strikingly similar to the hindbrain phenotype of *dreher* mutant mice harboring mutations in the *Lmx1a* gene (Manzanares et al., 2000; Millonig et al., 2000). During early embryonic development, the neural tube of *dreher* mutant mice is abnormally shaped due to failure to generate sufficient roof plate over the caudal hindbrain. Subsequent experiments have demonstrated that *Lmx1a* is both necessary and sufficient for roof plate induction in the spinal cord (Chizhikov et al., 2004b) and for 4th ventricle roof plate expansion in the hindbrain region (Chizhikov et al., submitted). *Lmx1b*, a closely related gene, shares at least some of this activity in spinal cord (Chizhikov et al., 2004c). In zebrafish, no *lmx1a* cDNA has been isolated, although two *lmx1b* duplicate genes have been described (O'Hara et al., 2005). A putative zebrafish *lmx1a* sequence does exist in the zebrafish genome database, but the failure to isolate a cDNA for this gene in the screening strategy described by O'Hara et al. (2005) implies that this gene is not abundant between 22-26hpf, and suggests that the duplicate *lmx1b* genes play the predominant role in zebrafish neural tube development. Consistent with this, we have shown that in zebrafish, the *lmx1b* duplicate genes play a similar function in roof plate development to mouse *Lmx1a*.

In Zic-deficient embryos we find both loss of morphologically identifiable roof plate and down-regulation or loss of dorsal midline *lmx1b* gene expression at different AP positions along the length of the hindbrain. We excluded the possibility that a mere delay in development can account for the loss of roof plate, as 48hpf Zic-deficient embryos also display a dorsal ventricle fused phenotype. We cannot formally distinguish between lack of roof plate as a consequence of disrupted Lmx1b function, versus a lack of *lmx1b* expression as a consequence of loss of roof plate. However, we noted that *lmx1b* reduction is the first observable defect in Zic morphants, preceding the initiation of roof plate expansion and ventricle opening by about two hours. In addition, we find that roof plate is absent or reduced in Lmx1b morphants, although interestingly, expanded *lmx1b* expression in response to loss of Wnt1 signals does not lead to an enlarged roof plate, showing that zebrafish Lmx1b is necessary but not sufficient for 4th ventricle roof plate development. A reasonable model to explain our results is that Zics function upstream of *lmx1b* genes to control roof plate development and ventricle opening. In support of this hypothesis, we find that partial knockdowns of Zic and Lmx genes cause synergistic phenotypes (Table 1). Reduced proliferation of roof plate progenitors, also under Zic control, may further contribute to the inability of roof plate to expand. While up-regulation of Zic1 and Zic4 expression has been reported in the dorsal spinal cord of *Lmx1b*^{-/-} mice (Ding et al., 2004), we have not observed altered *zic1* or *zic4* expression in the hindbrains of Lmx1b-deficient zebrafish, suggesting that context-dependent regulatory networks exist. As Lmx1b-deficient zebrafish show very similar ventricle defects to Zic-deficient zebrafish, we conclude that roof plate development is an integral component of 4th ventricle opening. A previous study reported that genetic ablation of roof plate from the mouse dorsal telencephalon similarly led to ventricle reduction (Cheng et al., 2006), suggesting that roof plate development is also critical to CNS morphogenesis at other levels along the AP axis.

A remaining unanswered question is the fate of those *Zic*-deficient cells that would normally contribute to the roof plate. As we do not detect elevated levels of apoptosis in *Zic*-deficient embryos, cell death cannot account for the loss of these cells. It is also unlikely that these cells acquire a ventral neural fate, as global DV patterning is not affected in *Zic* morphants (Fig. 4A-D). Rather, our results suggest that the most dorsal midline cells maintain dorsal (alar plate) character. We therefore suggest that the missing roof plate cells, which represent only a small cell population, likely contribute to an adjacent cell lineage; confirmation of this hypothesis must await detailed cell lineage tracing.

Rhombomere boundary patterning and hindbrain ventricle morphogenesis

Recent studies have documented the role of zebrafish rhombomere boundaries as signaling centers (Riley et al., 2004; Cheng et al., 2004, Amoyel and al. 2005). The generation of the appropriate number and types of mature neurons during early development requires temporal and spatial coordination of patterning, proliferation and differentiation, and Wnt factors expressed in signaling centers such as the roof plate have been demonstrated to play a role in these processes. Wnts have not only been shown to promote neural precursor proliferation in the spinal cord (Megason and McMahon, 2002; Zechner et al., 2003), but also to regulate neuronal differentiation in both the dorsal spinal cord (Muroyama et al., 2002; Zechner et al., 2007) and the zebrafish hindbrain (Amoyel et al., 2005). In zebrafish, in addition to their expression throughout the dorsal hindbrain, Wnt signals are expressed in two hindbrain signaling centers: in dorsal hindbrain boundaries and in the roof plate. Disruptions of rhombomere boundary formation, or of components of canonical Wnt signaling, have previously been associated with gross morphological defects in hindbrain ventricle shape (Amoyel et al., 2005). We have found that *Zic* morphants show reduced expression of *wnt1*, *wnt3a* and *wnt10*, specifically in rhombomere boundaries. We suggest that this loss of rhombomere boundary-derived signals has effects not only on neuronal proliferation and differentiation (as previously reported, Amoyel et al., 2005), but also on hindbrain ventricle opening.

Consistent with this hypothesis, we found that similar to *Zic1+4* knockdown, *Wnt1* knockdown led to ventricle fusion phenotypes. The complex expression of *wnts* obscures whether this knockdown phenotype is solely due to removing Wnt function in rhombomere boundaries, or if the dorsal expression of Wnts also plays a role in ventricle opening. However, we found that knockdown of *Rfng*, which disrupts Wnt function only in the boundaries (Cheng et al., 2004; Amoyel et al., 2005), again causes ventricle opening defects, suggesting that Wnt signals from rhombomere boundaries, independent of roof plate-derived signals, are critical to normal ventricle morphogenesis. Similarly, Dorsky et al. (2003) found that knockdown of *Tcf3b*, a downstream effector of Wnt signals, disrupted rhombomere boundary development and Amoyel et al. (2005) reported ventricle morphogenesis defects in both *Tcf3b* and *Wnt1* knockdowns. As *Zics* have previously been shown to induce *Wnt* expression in other species (Benedyk et al., 1994; Merzdorf and Sive, 2006), zebrafish *Zic1* and *Zic4* could potentially regulate rhombomere boundary *wnt* expression. Alternatively, the loss of *wnt* expression in rhombomere boundaries of *Zic* morphants may be an indirect consequence of loss of roof plate-derived signals. Interestingly, 52% of *Lmx1b*-deficient embryos show down-regulation of *wnt1* expression in rhombomere boundaries, supporting the hypothesis that roof plate-derived signals regulate Wnt expression in rhombomere boundaries. This ability of *Lmx1b* to influence *wnt* expression in rhombomere boundaries may in turn be dependent on direct *Lmx1b* regulation of *wnt* expression in the roof plate. Several lines of evidence show that *Lmx1b* has the capacity to regulate *wnt* gene expression. *Wnt1* expression in the midbrain/hindbrain isthmus is lost both in *Lmx1b* mutant mice (Guo et al., 2007) and in *Lmx1b.1 + Lmx1b.2* zebrafish morphants (O'Hara et al., 2005). In addition, mis-expression of *Lmx1b* in zebrafish hindbrain leads to ectopic expression of *wnt1* (O'Hara et al., 2005). These findings, taken

together with our own data, suggest that *lmx1b* genes may similarly regulate *wnt* expression in the hindbrain roof plate. In summary, our results indicate that roof plate-derived signals are necessary to maintain rhombomere boundary signaling centers, and that once formed, the boundary signaling centers themselves play a critical role in ventricle morphogenesis independent of roof plate-derived signaling.

Multiple mechanisms are required for ventricle development

Our results are consistent with a model in which input from multiple signaling pathways is required both temporally and spatially for ventricle morphogenesis. Previous studies have indicated that the shape of the hindbrain ventricle is influenced via a wide variety of mechanisms. These include correct neuronal patterning and positional information (Bae et al., 2005; Bingham et al., 2003; Mawdsley et al., 2004; Schier et al., 1996), localized cell-cell interactions and cell-shape changes (Hong and Brewster, 2006; Lele et al., 2002), cell proliferation (Lowery and Sive, 2005; Nyholm et al., 2007; Song et al., 2004), ion transport into the ventricular space (Lowery and Sive, 2005), and proper cellular polarity/integrity of the neuroepithelium prior to ventricle opening (Lowery and Sive, 2005). Our experiments have revealed that *Zic1* and *Zic4* also play a critical role in controlling 4th ventricle development. We have established that the role of these transcription factors in this process is via integration of their complex pleiotropic functions in controlling dorsal neural proliferation and dorsal hindbrain development, including roof plate formation.

Supplementary Material

Refer to Web version on PubMed Central for supplementary material.

ACKNOWLEDGEMENTS

We would like to thank M. Gillhouse for cloning the *zic4* gene, and M. Rowe for expert assistance with fish care. We thank C. Thisse for providing the *gdf6a* clone, D. Kessler for the *lmx1b.1* clone and morpholinos to *Lmx1b.1* and *Lmx1b.2*, D. Wilkinson for the *rfg* clone, A. Fjose for *pax3* and *pax7* clones, L. Bally-Cuif for the *atoh1.2* clone, and D. Ahn for the *lmx1b.2* clone. We are also very grateful to W. Dobyns for his support and E. Grove and R. Ho for discussions on this study. This work was supported by Institutional Training Grant T32 GM07839, and by NIH grant NS050386 to KM.

REFERENCES

- Adolf B, Bellipanni G, Huber V, Bally-Cuif L. *atoh1.2* and *beta3.1* are two new bHLH-encoding genes expressed in selective precursor cells of the zebrafish anterior hindbrain. *Gene Expr Patterns* 2004;5:35–41. [PubMed: 15533816]
- Akimenko MA, Ekker M, Wegner J, Lin W, Westerfield M. Combinatorial expression of three zebrafish genes related to *distal-less*: part of a homeobox gene code for the head. *J Neurosci* 1994;14:3475–86. [PubMed: 7911517]
- Amoyel M, Cheng YC, Jiang YJ, Wilkinson DG. *Wnt1* regulates neurogenesis and mediates lateral inhibition of boundary cell specification in the zebrafish hindbrain. *Development* 2005;132:775–85. [PubMed: 15659486]
- Aruga J. The role of *Zic* genes in neural development. *Mol Cell Neurosci* 2004;26:205–21. [PubMed: 15207846]
- Aruga J, Inoue T, Hoshino J, Mikoshiba K. *Zic2* controls cerebellar development in cooperation with *Zic1*. *J Neurosci* 2002a;22:218–25. [PubMed: 11756505]
- Aruga J, Minowa O, Yaginuma H, Kuno J, Nagai T, Noda T, Mikoshiba K. Mouse *Zic1* is involved in cerebellar development. *J Neurosci* 1998;18:284–93. [PubMed: 9412507]
- Aruga J, Tohmonda T, Homma S, Mikoshiba K. *Zic1* promotes the expansion of dorsal neural progenitors in spinal cord by inhibiting neuronal differentiation. *Dev Biol* 2002b;244:329–41. [PubMed: 11944941]

- Bae YK, Shimizu T, Hibi M. Patterning of proneuronal and inter-proneuronal domains by hairy- and enhancer of split-related genes in zebrafish neuroectoderm. *Development* 2005;132:1375–85. [PubMed: 15716337]
- Benedyk MJ, Mullen JR, DiNardo S. odd-paired: a zinc finger pair-rule protein required for the timely activation of engrailed and wingless in *Drosophila* embryos. *Genes Dev* 1994;8:105–17. [PubMed: 8288124]
- Bergsneider M, Egnor MR, Johnston M, Kranz D, Madsen JR, McAllister JP 2nd, Stewart C, Walker ML, Williams MA. What we don't (but should) know about hydrocephalus. *J Neurosurg* 2006;104:157–9. [PubMed: 16572631]
- Bingham S, Chaudhari S, Vanderlaan G, Itoh M, Chitnis A, Chandrasekhar A. Neurogenic phenotype of mind bomb mutants leads to severe patterning defects in the zebrafish hindbrain. *Dev Dyn* 2003;228:451–63. [PubMed: 14579383]
- Brewster R, Lee J, Ruiz i Altaba A. Gli/Zic factors pattern the neural plate by defining domains of cell differentiation. *Nature* 1998;393:579–83. [PubMed: 9634234]
- Brown LY, Odent S, David V, Blayau M, Dubourg C, Apacik C, Delgado MA, Hall BD, Reynolds JF, Sommer A, Wieczorek D, Brown SA, Muenke M. Holoprosencephaly due to mutations in ZIC2: alanine tract expansion mutations may be caused by parental somatic recombination. *Hum Mol Genet* 2001;10:791–6. [PubMed: 11285244]
- Cheng X, Hsu CM, Currie DS, Hu JS, Barkovich AJ, Monuki ES. Central roles of the roof plate in telencephalic development and holoprosencephaly. *J Neurosci* 2006;26:7640–9. [PubMed: 16855091]
- Cheng YC, Amoyel M, Qiu X, Jiang YJ, Xu Q, Wilkinson DG. Notch activation regulates the segregation and differentiation of rhombomere boundary cells in the zebrafish hindbrain. *Dev Cell* 2004;6:539–50. [PubMed: 15068793]
- Chizhikov VV, Millen KJ. Mechanisms of roof plate formation in the vertebrate CNS. *Nat Rev Neurosci* 2004a;5:808–12. [PubMed: 15378040]
- Chizhikov VV, Millen KJ. Control of roof plate development and signaling by Lmx1b in the caudal vertebrate CNS. *J Neurosci* 2004b;24:5694–703. [PubMed: 15215291]
- Chizhikov VV, Millen KJ. Control of roof plate formation by Lmx1a in the developing spinal cord. *Development* 2004c;131:2693–705. [PubMed: 15148302]
- Chizhikov VV, Millen KJ. Roof plate-dependent patterning of the vertebrate dorsal central nervous system. *Dev Biol* 2005;277:287–95. [PubMed: 15617675]
- Ciruna B, Jenny A, Lee D, Mlodzik M, Schier AF. Planar cell polarity signalling couples cell division and morphogenesis during neurulation. *Nature* 2006;439:220–4. [PubMed: 16407953]
- Concha ML, Adams RJ. Oriented cell divisions and cellular morphogenesis in the zebrafish gastrula and neurula: a time-lapse analysis. *Development* 1998;125:983–94. [PubMed: 9463345]
- Davidson AJ, Postlethwait JH, Yan YL, Beier DR, van Doren C, Foernzler D, Celeste AJ, Crosier KE, Crosier PS. Isolation of zebrafish *gdf7* and comparative genetic mapping of genes belonging to the growth/differentiation factor 5, 6, 7 subgroup of the TGF-beta superfamily. *Genome Res* 1999;9:121–9. [PubMed: 10022976]
- Ding YQ, Yin J, Kania A, Zhao ZQ, Johnson RL, Chen ZF. Lmx1b controls the differentiation and migration of the superficial dorsal horn neurons of the spinal cord. *Development* 2004;131:3693–703. [PubMed: 15229182]
- Dorsky RI, Itoh M, Moon RT, Chitnis A. Two *tcf3* genes cooperate to pattern the zebrafish brain. *Development* 2003;130:1937–47. [PubMed: 12642497]
- Fujimi TJ, Mikoshiba K, Aruga J. *Xenopus Zic4*: conservation and diversification of expression profiles and protein function among the *Xenopus Zic* family. *Dev Dyn* 2006;235:3379–86. [PubMed: 16871625]
- Geldmacher-Voss B, Reugels AM, Pauls S, Campos-Ortega JA. A 90-degree rotation of the mitotic spindle changes the orientation of mitoses of zebrafish neuroepithelial cells. *Development* 2003;130:3767–80. [PubMed: 12835393]
- Grinberg I, Millen KJ. The ZIC gene family in development and disease. *Clin Genet* 2005;67:290–6. [PubMed: 15733262]

- Grinberg I, Northrup H, Ardinger H, Prasad C, Dobyns WB, Millen KJ. Heterozygous deletion of the linked genes ZIC1 and ZIC4 is involved in Dandy-Walker malformation. *Nat Genet* 2004;36:1053–5. [PubMed: 15338008]
- Grinblat Y, Gamse J, Patel M, Sive H. Determination of the zebrafish forebrain: induction and patterning. *Development* 1998;125:4403–16. [PubMed: 9778500]
- Grinblat Y, Sive H. zic Gene expression marks anteroposterior pattern in the presumptive neurectoderm of the zebrafish gastrula. *Dev Dyn* 2001;222:688–93. [PubMed: 11748837]
- Guo C, Qiu HY, Huang Y, Chen H, Yang RQ, Chen SD, Johnson RL, Chen ZF, Ding YQ. Lmx1b is essential for Fgf8 and Wnt1 expression in the isthmic organizer during tectum and cerebellum development in mice. *Development* 2007;134:317–25. [PubMed: 17166916]
- Hong E, Brewster R. N-cadherin is required for the polarized cell behaviors that drive neurulation in the zebrafish. *Development* 2006;133:3895–905. [PubMed: 16943271]
- Irving C, Flenniken A, Alldus G, Wilkinson DG. Cell-cell interactions and segmentation in the developing vertebrate hindbrain. *Biochem Soc Symp* 1996;62:85–95. [PubMed: 8971342]
- Jiang YJ, Brand M, Heisenberg CP, Beuchle D, Furutani-Seiki M, Kelsh RN, Warga RM, Granato M, Haffter P, Hammerschmidt M, Kane DA, Mullins MC, Odenthal J, van Eeden FJ, Nusslein-Volhard C. Mutations affecting neurogenesis and brain morphology in the zebrafish, *Danio rerio*. *Development* 1996;123:205–16. [PubMed: 9007241]
- Kahane N, Kalcheim C. Identification of early postmitotic cells in distinct embryonic sites and their possible roles in morphogenesis. *Cell Tissue Res* 1998;294:297–307. [PubMed: 9799446]
- Keller MJ, Chitnis AB. Insights into the evolutionary history of the vertebrate zic3 locus from a teleost-specific zic6 gene in the zebrafish, *Danio rerio*. *Dev Genes Evol* 2007;217:541–7. [PubMed: 17503076]
- Kimmel CB, Ballard WW, Kimmel SR, Ullmann B, Schilling TF. Stages of embryonic development of the zebrafish. *Dev Dyn* 1995;203:253–310. [PubMed: 8589427]
- Kimmel CB, Warga RM, Kane DA. Cell cycles and clonal strings during formation of the zebrafish central nervous system. *Development* 1994;120:265–76. [PubMed: 8149908]
- Koster RW, Fraser SE. Direct imaging of in vivo neuronal migration in the developing cerebellum. *Curr Biol* 2001;11:1858–63. [PubMed: 11728308]
- Krauss S, Concordet JP, Ingham PW. A functionally conserved homolog of the *Drosophila* segment polarity gene hh is expressed in tissues with polarizing activity in zebrafish embryos. *Cell* 1993;75:1431–44. [PubMed: 8269519]
- Lele Z, Folchert A, Concha M, Rauch GJ, Geisler R, Rosa F, Wilson SW, Hammerschmidt M, Bally-Cuif L. parachute/n-cadherin is required for morphogenesis and maintained integrity of the zebrafish neural tube. *Development* 2002;129:3281–94. [PubMed: 12091300]
- Lowery LA, Sive H. Strategies of vertebrate neurulation and a re-evaluation of teleost neural tube formation. *Mech Dev* 2004;121:1189–97. [PubMed: 15327780]
- Lowery LA, Sive H. Initial formation of zebrafish brain ventricles occurs independently of circulation and requires the nagie oko and snakehead/atp1a1a.1 gene products. *Development* 2005;132:2057–67. [PubMed: 15788456]
- Lyons DA, Guy AT, Clarke JD. Monitoring neural progenitor fate through multiple rounds of division in an intact vertebrate brain. *Development* 2003;130:3427–36. [PubMed: 12810590]
- Manzanares M, Trainor PA, Ariza-McNaughton L, Nonchev S, Krumlauf R. Dorsal patterning defects in the hindbrain, roof plate and skeleton in the dreher (dr(J)) mouse mutant. *Mech Dev* 2000;94:147–56. [PubMed: 10842066]
- Mawdsley DJ, Cooper HM, Hogan BM, Cody SH, Lieschke GJ, Heath JK. The Netrin receptor Neogenin is required for neural tube formation and somitogenesis in zebrafish. *Dev Biol* 2004;269:302–15. [PubMed: 15081375]
- McAllister JP 2nd, Chovan P. Neonatal hydrocephalus. Mechanisms and consequences. *Neurosurg Clin N Am* 1998;9:73–93. [PubMed: 9405766]
- McClintock JM, Carlson R, Mann DM, Prince VE. Consequences of Hox gene duplication in the vertebrates: an investigation of the zebrafish Hox paralogue group 1 genes. *Development* 2001;128:2471–84. [PubMed: 11493564]

- Megason SG, McMahon AP. A mitogen gradient of dorsal midline Wnts organizes growth in the CNS. *Development* 2002;129:2087–98. [PubMed: 11959819]
- Mellitzer G, Xu Q, Wilkinson DG. Eph receptors and ephrins restrict cell intermingling and communication. *Nature* 1999;400:77–81. [PubMed: 10403252]
- Merzdorf CS. Emerging roles for zic genes in early development. *Dev Dyn* 2007;236:922–940. [PubMed: 17330889]
- Merzdorf CS, Sive HL. The zic1 gene is an activator of Wnt signaling. *Int J Dev Biol* 2006;50:611–7. [PubMed: 16892174]
- Millonig JH, Millen KJ, Hatten ME. The mouse Dreher gene Lmx1a controls formation of the roof plate in the vertebrate CNS. *Nature* 2000;403:764–9. [PubMed: 10693804]
- Miyan JA, Nabiyouni M, Zendah M. Development of the brain: a vital role for cerebrospinal fluid. *Can J Physiol Pharmacol* 2003;81:317–28. [PubMed: 12769224]
- Moens CB, Prince VE. Constructing the hindbrain: insights from the zebrafish. *Dev Dyn* 2002;224:1–17. [PubMed: 11984869]
- Muroyama Y, Fujihara M, Ikeya M, Kondoh H, Takada S. Wnt signaling plays an essential role in neuronal specification of the dorsal spinal cord. *Genes Dev* 2002;16:548–53. [PubMed: 11877374]
- Nagai T, Aruga J, Minowa O, Sugimoto T, Ohno Y, Noda T, Mikoshiba K. Zic2 regulates the kinetics of neurulation. *Proc Natl Acad Sci U S A* 2000;97:1618–23. [PubMed: 10677508]
- Nakata K, Koyabu Y, Aruga J, Mikoshiba K. A novel member of the Xenopus Zic family, Zic5, mediates neural crest development. *Mech Dev* 2000;99:83–91. [PubMed: 11091076]
- Nakata K, Nagai T, Aruga J, Mikoshiba K. Xenopus Zic family and its role in neural and neural crest development. *Mech Dev* 1998;75:43–51. [PubMed: 9739105]
- Nasevicius A, Ekker SC. Effective targeted gene ‘knockdown’ in zebrafish. *Nat Genet* 2000;26:216–20. [PubMed: 11017081]
- Novak Z, Krupa P, Zlatos J, Nadvornik P. The function of the cerebrospinal fluid space and its expansion. *Bratisl Lek Listy* 2000;101:594–7. [PubMed: 11218955]
- Nyholm MK, Wu SF, Dorsky RI, Grinblat Y. The zebrafish zic2a-zic5 gene pair acts downstream of canonical Wnt signaling to control cell proliferation in the developing tectum. *Development* 2007;134:735–46. [PubMed: 17215296]
- O’Hara FP, Beck E, Barr LK, Wong LL, Kessler DS, Riddle RD. Zebrafish Lmx1b.1 and Lmx1b.2 are required for maintenance of the isthmus organizer. *Development* 2005;132:3163–73. [PubMed: 15944182]
- Oxtoby E, Jowett T. Cloning of the zebrafish krox-20 gene (krx-20) and its expression during hindbrain development. *Nucleic Acids Res* 1993;21:1087–95. [PubMed: 8464695]
- Papan C, Campos-Ortega JA. On the formation of the neural keel and neural tube in the zebrafish *Danio (braquydanio) rerio*. *Roux’s Arch. Dev. Biol* 1994;203:178–198.
- Phillips BT, Kwon HJ, Melton C, Houghtaling P, Fritz A, Riley BB. Zebrafish msxB, msxC and msxE function together to refine the neural-non-neural border and regulate cranial placodes and neural crest development. *Dev Biol* 2006;294:376–90. [PubMed: 16631154]
- Prince VE, Moens CB, Kimmel CB, Ho RK. Zebrafish hox genes: expression in the hindbrain region of wild-type and mutants of the segmentation gene, valentino. *Development* 1998;125:393–406. [PubMed: 9425135]
- Riley BB, Chiang MY, Storch EM, Heck R, Buckles GR, Lekven AC. Rhombomere boundaries are Wnt signaling centers that regulate metameric patterning in the zebrafish hindbrain. *Dev Dyn* 2004;231:278–91. [PubMed: 15366005]
- Rohr KB, Schulte-Merker S, Tautz D. Zebrafish zic1 expression in brain and somites is affected by BMP and hedgehog signalling. *Mech Dev* 1999;85:147–59. [PubMed: 10415355]
- Schier AF, Neuhauss SC, Harvey M, Malicki J, Solnica-Krezel L, Stainier DY, Zwartkruis F, Abdelilah S, Stemple DL, Rangini Z, Yang H, Driever W. Mutations affecting the development of the embryonic zebrafish brain. *Development* 1996;123:165–78. [PubMed: 9007238]
- Schmitz B, Papan C, Campos-Ortega JA. Neurulation in the anterior trunk region of the zebrafish *Bracydanio rerio*. *Roux’s Arch. Dev. Biol* 1993;202:250–259.

- Seo HC, Saetre BO, Havik B, Ellingsen S, Fjose A. The zebrafish Pax3 and Pax7 homologues are highly conserved, encode multiple isoforms and show dynamic segment-like expression in the developing brain. *Mech Dev* 1998;70:49–63. [PubMed: 9510024]
- Shepard JL, Stern HM, Pfaff KL, Amatruda JF. Analysis of the cell cycle in zebrafish embryos. *Methods Cell Biol* 2004;76:109–25. [PubMed: 15602874]
- Song MH, Brown NL, Kuwada JY. The cfy mutation disrupts cell divisions in a stage-dependent manner in zebrafish embryos. *Dev Biol* 2004;276:194–206. [PubMed: 15531374]
- Stewart RA, Arduini BL, Berghmans S, George RE, Kanki JP, Henion PD, Look AT. Zebrafish foxd3 is selectively required for neural crest specification, migration and survival. *Dev Biol* 2006;292:174–88. [PubMed: 16499899]
- Tawk M, Araya C, Lyons DA, Reugels AM, Girdler GC, Bayley PR, Hyde DR, Tada M, Clarke JD. A mirror-symmetric cell division that orchestrates neuroepithelial morphogenesis. *Nature*. 2007
- Thisse B, Pflumio S, Fürthauer M, Loppin B, Heyer V, Degraeve A, Woehl R, Lux A, Steffan T, Charbonnier XQ, Thisse C. Expression of the zebrafish genome during embryogenesis (NIH R01 RR15402). ZFIN Direct Data Submission. 2001
- Trevarrow B, Marks DL, Kimmel CB. Organization of hindbrain segments in the zebrafish embryo. *Neuron* 1990;4:669–79. [PubMed: 2344406]
- Wiellette E, Grinblat Y, Austen M, Hirsinger E, Amsterdam A, Walker C, Westerfield M, Sive H. Combined haploid and insertional mutation screen in the zebrafish. *Genesis* 2004;40:231–40. [PubMed: 15593329]
- Wurst W, Bally-Cuif L. Neural plate patterning: upstream and downstream of the isthmic organizer. *Nat Rev Neurosci* 2001;2:99–108. [PubMed: 11253000]
- Zechner D, Fujita Y, Hulsken J, Muller T, Walther I, Taketo MM, Crenshaw EB 3rd, Birchmeier W, Birchmeier C. beta-Catenin signals regulate cell growth and the balance between progenitor cell expansion and differentiation in the nervous system. *Dev Biol* 2003;258:406–18. [PubMed: 12798297]
- Zechner D, Muller T, Wende H, Walther I, Taketo MM, Crenshaw EB 3rd, Treier M, Birchmeier W, Birchmeier C. Bmp and Wnt/beta-catenin signals control expression of the transcription factor Olig3 and the specification of spinal cord neurons. *Dev Biol* 2007;303:181–90. [PubMed: 17150208]
- Zhao ZQ, Scott M, Chiechio S, Wang JS, Renner KJ, Gereau R. W. t. Johnson RL, Deneris ES, Chen ZF. Lmx1b is required for maintenance of central serotonergic neurons and mice lacking central serotonergic system exhibit normal locomotor activity. *J Neurosci* 2006;26:12781–8. [PubMed: 17151281]

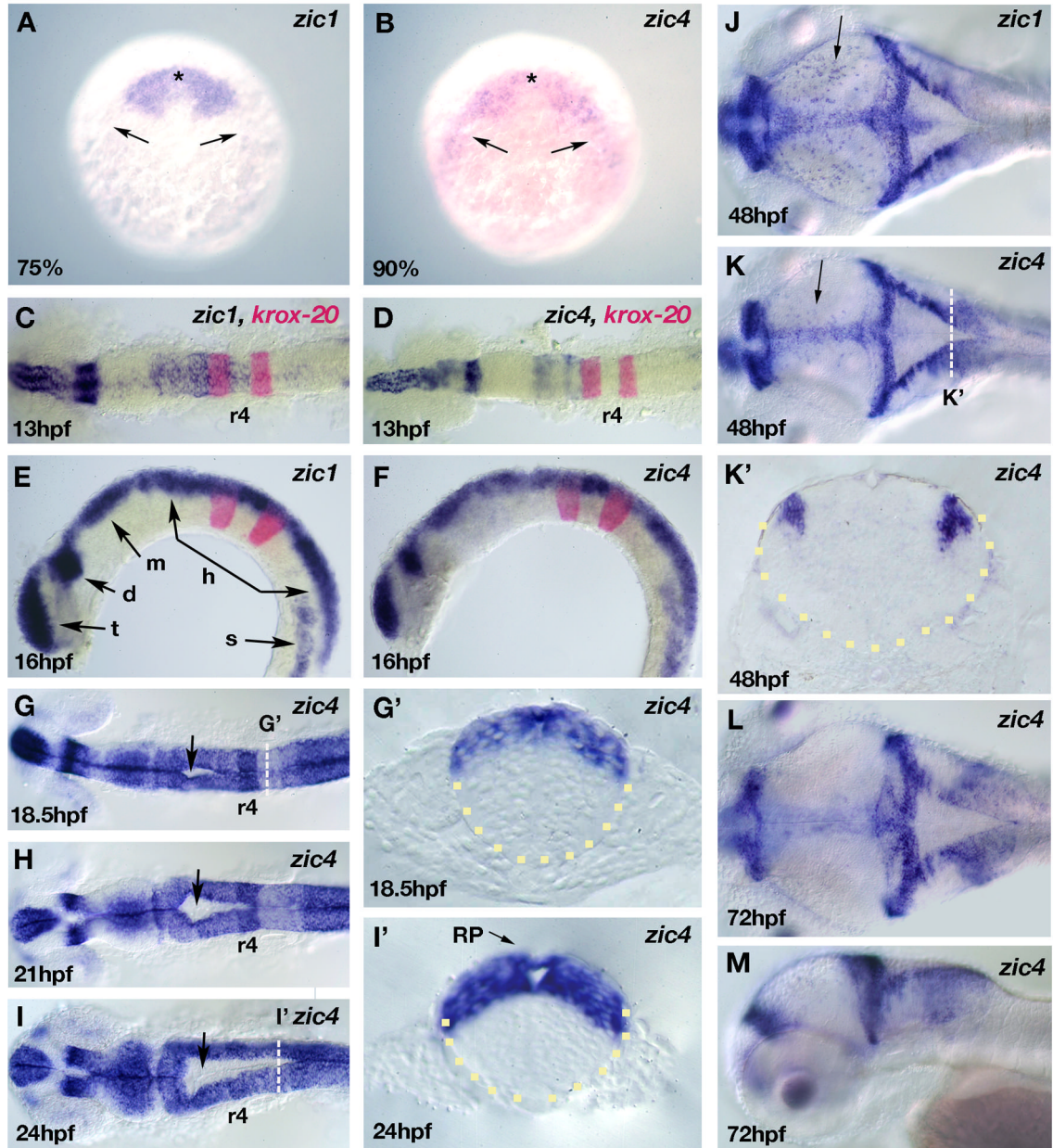


Fig. 1. Dorsal neural tube restriction of *zic1* and *zic4* linked genes during embryonic development (A,B) Dorsal view (anterior to the top) of RNA *in situ* hybridization of *zic1* (A) and *zic4* (B) at their onset of expression at 75% epiboly (*zic1*) and 90% epiboly (*zic4*) in the anterior (asterisks) and lateral border (arrows) of the neural plate. (C-M) Developmental stages are as indicated; dorsal (C,D,G,H,I,J,K,L) and lateral (E,F,M) views, anterior to the left. Transverse sections of the neural tube (outlined with yellow dots) (G',I',K'). (C-F) Whole-mount embryos showing modulated *zic1* (C,E) and *zic4* (D,F) expression along the AP axis (C,D) and dorsal restriction of expression in the neural tube (E,F). (C-F) *krox20* is a marker for r3 and r5. (G-I) *zic4* RNA *in situ* hybridization of whole-mount embryos highlighting the progression of hindbrain ventricle opening (arrows) from 18.5hpf (G) to 21hpf (H) and 24hpf (I). Note dorsal restriction of *zic4* expression in transverse sections through r5 at 18.5hpf (G') and 24hpf (I'), as indicated by white dotted lines in G and I respectively. Note at 18.5hpf (G') the absence of

a ventricle opening, while at 24hpf (I') the opening is clearly defined. Zic4 is expressed in the roof plate (RP) indicated by arrow in I'. (J-M) *zic1* (J) and *zic4* (K,L,M) transcripts continue to be expressed in the dorsal neural tube. Arrow in J and K indicates the expression of *zic1* and *zic4* respectively in an unidentified population of dorsal midbrain neurons. Dorso-lateral expression domain of *zic4* is maintained at 48hpf (K') in transverse section at level indicated by white dotted line in K. t, telencephalon; d, diencephalon; m, midbrain; h, hindbrain, s, somites

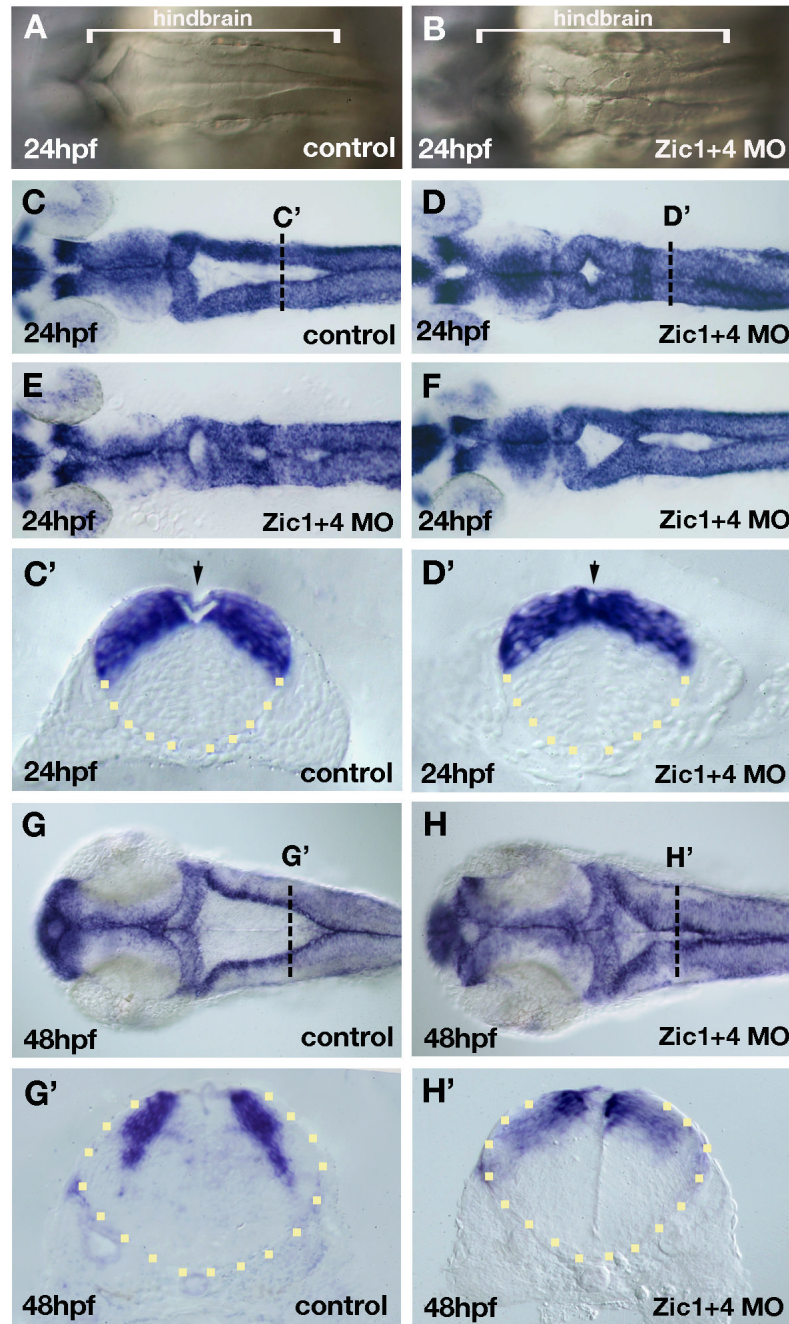


Fig. 2. Dorsal hindbrain ventricle morphogenesis is altered in *Zic1* and *Zic4* morphants
 Dorsal view of the hindbrain (A-F,G,H) and cross-sections of the neural tube (outlined by yellow dots) at the level of r5 (C',D',G',H'). (A,B) Bright field live images of hindbrains of 24hpf control embryos (A) and *Zic1+4* morphants (B). Dorsal folds that outline the hindbrain ventricle in control hindbrains (A) are aberrantly fused at the dorsal midline in *Zic1+4* morphants (B). Brackets in A and B indicate the length of the hindbrain.(C-F) Dorsal *zic1* expression at 24hpf allows visualization of hindbrain ventricle defects in *Zic1+4* morphants (D-F; and see Table 1) compared to controls (C). Transverse sections at AP levels indicated by white dotted lines in C and D show hindbrain ventricle opening is impaired in 24hpf *Zic1+4* morphants (D') compared to controls (C'). Arrow in C' indicates roof plate (RP) overlying

the ventricle, and in D' indicates absence of a well-defined RP. (G-H') Dorsal view of *zic1* expression in 48hpf controls (G) and *Zic1+4* morphants (H) showing "dorsal fused" phenotype. (G',H') Transverse sections at AP levels indicated by the white dotted lines in G and H show ventricle opening is impaired in 48hpf *Zic1+4* morphants (H') compared to controls (G').

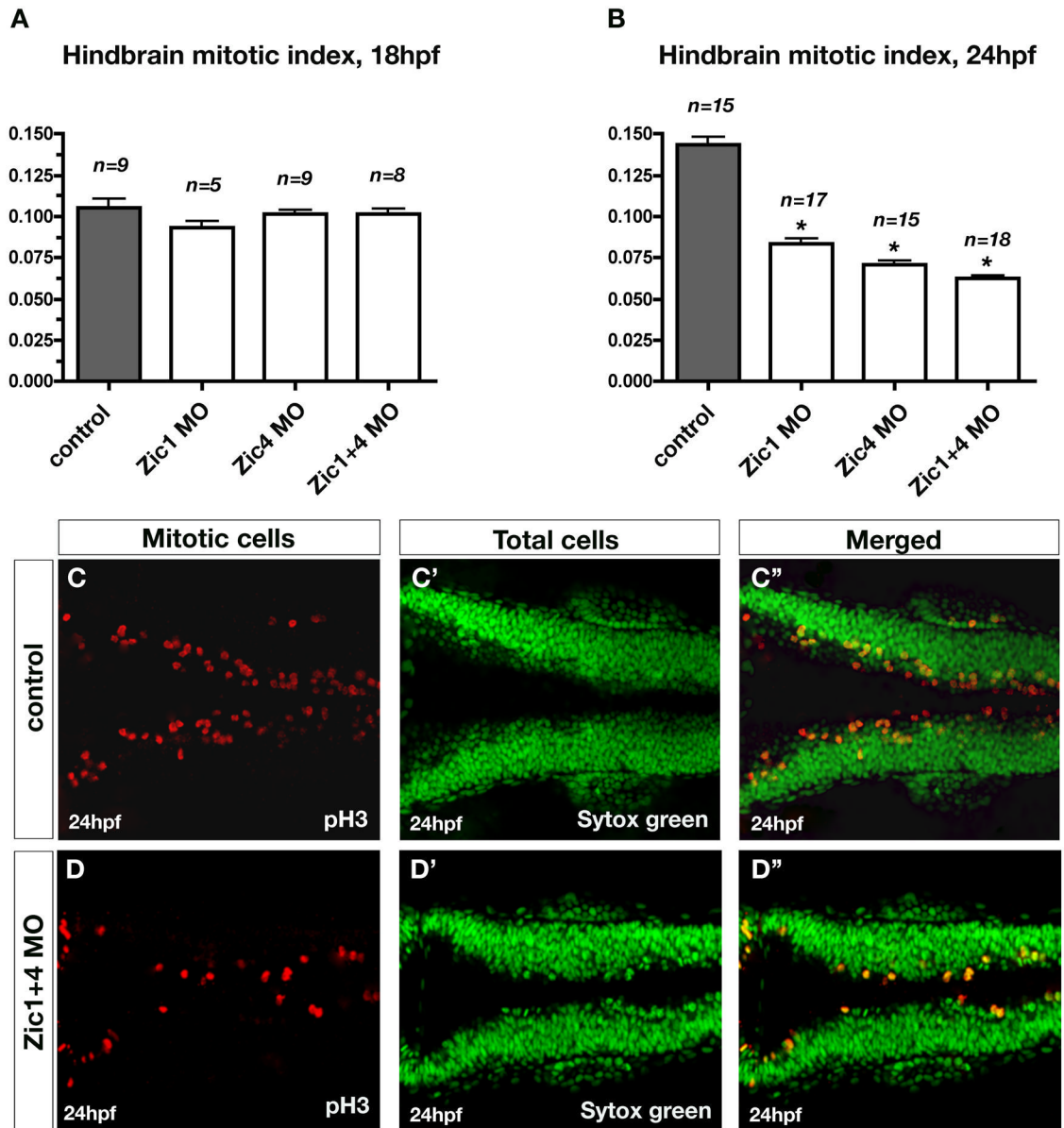


Fig. 3. Zic1 and Zic4 function is required after initial ventricle opening for dorsal neural proliferation in the hindbrain

(A,B) Comparison of the quantitative analysis of hindbrain mitotic index at 18hpf (A) and 24hpf (B) in controls, Zic1 morphants, Zic4 morphants, and Zic1+4 morphants. Mitotic index was calculated in controls and Zic morphants as the ratio of the number of proliferating cells over the total number of cells (as described in Methods). Dorsal neural proliferation at 18hpf remained unaffected in Zic morphants compared to controls (A), while at 24hpf the mitotic index was reduced in Zic morphants compared to controls (B). n is the number of embryos assessed per experimental condition. Asterisks (in B) indicate significant differences compared to controls. (C,D) Dorsal confocal sections (3 μ m thick; longitudinal view) through hindbrain immunolabeled with the proliferating marker pH3 (C,D), counterstained with the nuclear marker Sytox green (C',D'), and merged (C'',D'') of 24hpf controls (C,C',C'') and Zic1+4 morphants (D,D',D'').

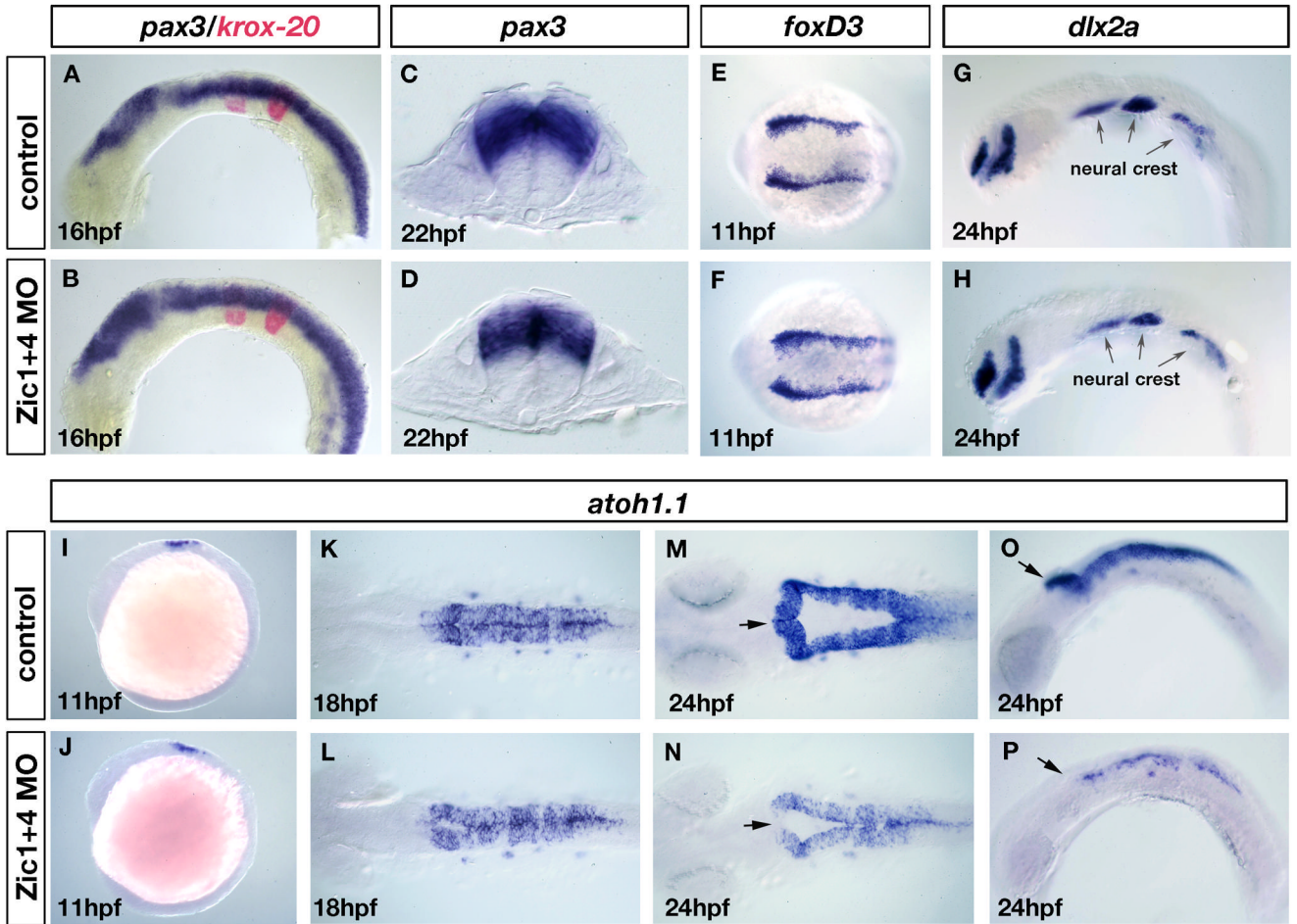


Fig. 4. Dorsal fates are selectively altered in *Zic1* and *Zic4* morphants without affecting early dorsal-ventral (DV) or anterior-posterior (AP) patterning

(A-D) RNA *in situ* hybridization with a DV marker *pax3* (blue in A-D) and an AP marker *krox20* (red in A,B). Lateral view of 16hpf embryos (A,B) and transverse sections at the level of r5 of 22hpf embryos (C,D). DV and AP marker distribution and expression are established normally in *Zic1+4* morphants (B,D) compared to controls (A,C). (E-H) Dorsal view of 11hpf embryos labeled with the early neural crest induction/specification marker *foxD3* (E,F) and lateral view of 24hpf embryos labeled with a neural crest migration marker *dlx2a* (G,H). Arrows in G and H indicate the expression of *dlx2a* in the pharyngeal arches. Neural crest induction and migration is unaltered in *Zic1+4* morphants (F,H) compared to controls (E,G). (I-P) *atoh1.1* expression labels dorsal hindbrain progenitors, stages as indicated: lateral views (I,J,O,P), and dorsal views (K-N). At 11hpf *atoh1.1* expression is unaffected in *Zic1+4* morphants (J) compared to controls (I). At 18hpf expression is slightly reduced in *Zic1+4* morphants (L) compared to controls (K). By 24hpf *atoh1.1* expression levels and domain size are dramatically reduced in *Zic1+4* morphants (N, P) compared to controls (M, O). Arrows in M-P indicate the anterior region of r1, where expression of *atoh1.1* is lost in *Zic1+4* morphants.

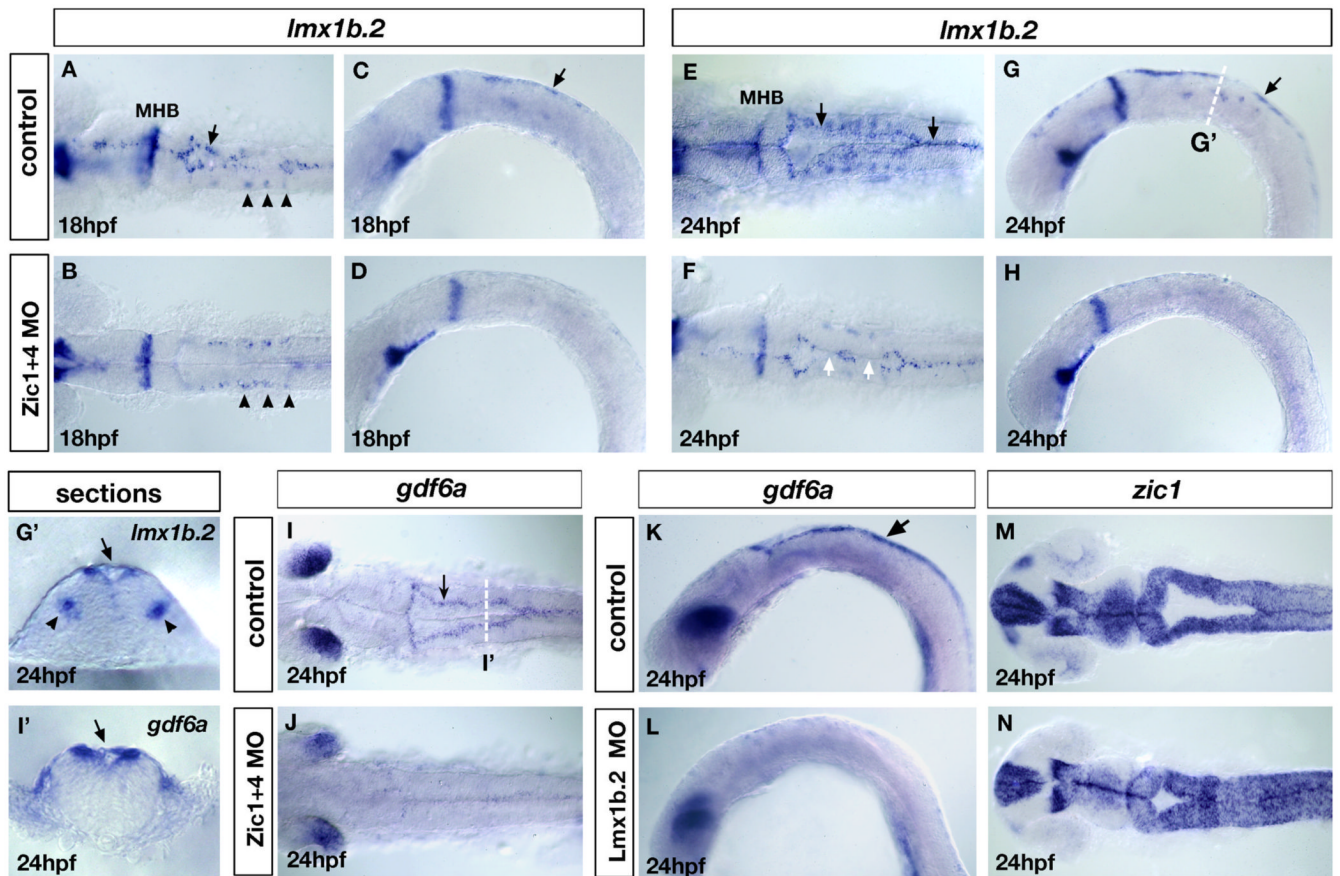


Fig. 5. Loss of *lmx1b* expression in *Zic* morphants underlies loss of roof plate development and is linked to ventricle morphogenesis

(A-H) Expression of *lmx1b.2* at 18hpf (A-D) and 24hpf (E-H). Dorsal view (A,B and E,F) and lateral view (C,D and G,H) of controls (A,C and E,G) and *Zic1+4* morphants (B,D and F,H). In *Zic1+4* morphants, the expression of *lmx1b.2* in hindbrain roof plate (RP) is missing or down-regulated in 18hpf (B,D) and 24hpf embryos (F,H) compared to controls at 18hpf (A,C) and 24hpf (E,G). The expression of *lmx1b.2* in roof plate is indicated in controls (A,C and E,G) by black arrows. The expression of *lmx1b.2* in ventral serotonergic neurons is unaffected in *Zic1+4* morphants (arrowheads in A,B). In 24hpf *Zic1+4* morphants, loss of *lmx1b.2* expression in the roof plate correlates with points of dorsal fusion (white arrows in F). (G',I') Cross-sections at the levels indicated in G and I of 24hpf embryos labeled with *lmx1b.2* probes (G') and *gdf6a* probes (I') to illustrate their expression in roof plate cells (indicated by black arrows). The expression of *lmx1b.2* in ventral serotonergic neurons is indicated by black arrowheads. (I,J) *gdf6a* expression in dorsal view of 24hpf controls (I) and *Zic1+4* morphants (J). In control embryos, *gdf6a* is expressed in the roof plate (arrow in I). In *Zic1+4* morphants (J), the expression of *gdf6a* expression is missing or down-regulated in roof plate compared to controls (I). (K,L) *gdf6a* expression in 24hpf lateral view control embryos (arrow in K indicates expression in the RP) and *Lmx1b.2* morphants (L), shows that *gdf6a* expression in roof plate is missing or down-regulated (L). (M,N) *zic1* expression, dorsal view of 24hpf controls (M) and *Lmx1b.2* morphants (N) shows that *Lmx1b.2* knockdown causes a dorsal ventricle fusion phenotype. MHB, midbrain-hindbrain boundary.

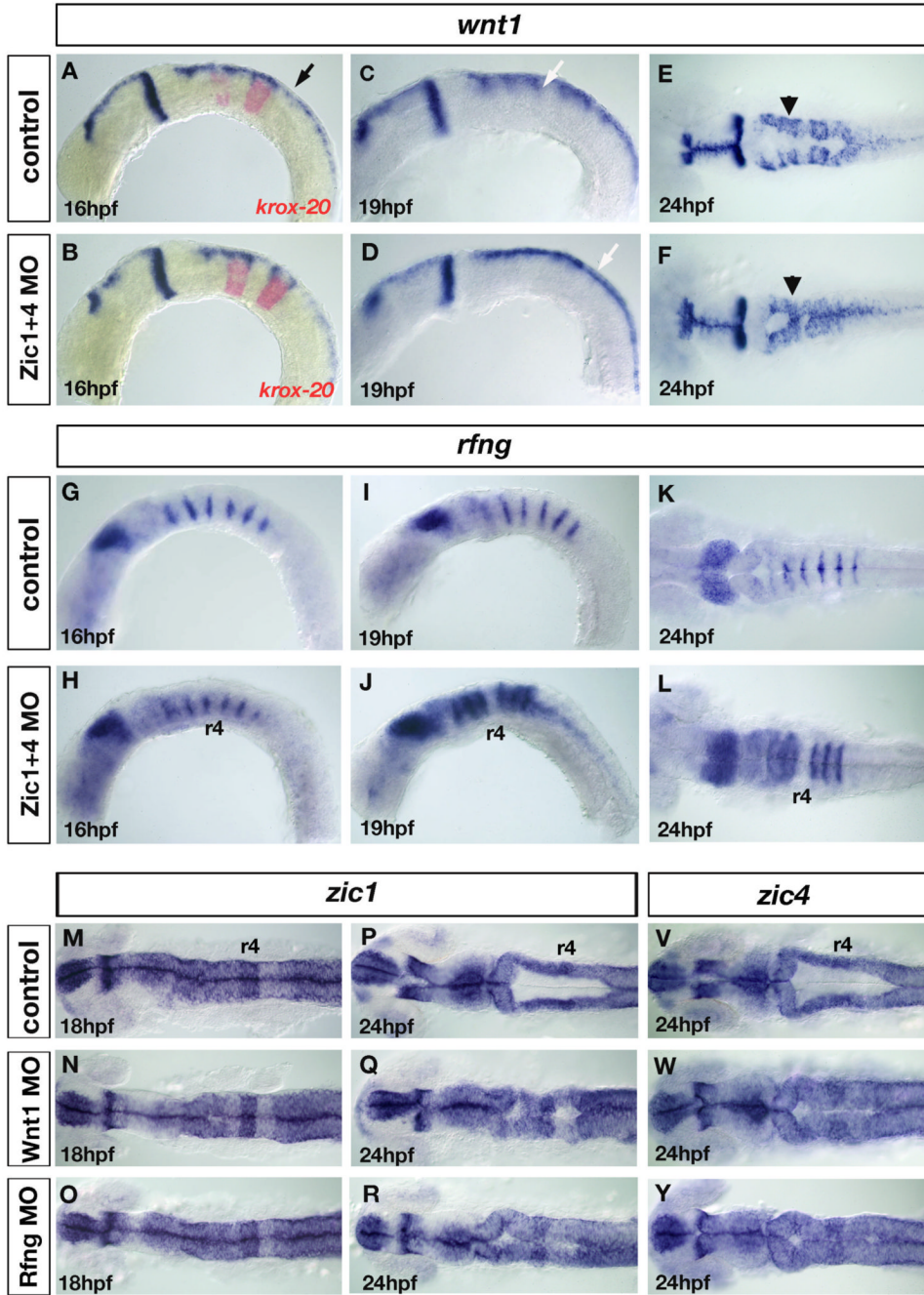


Fig. 6. Loss of *wnt* signaling centers at the rhombomere boundaries in *Zic1* and *Zic4* morphants affects ventricle morphogenesis
 (A-F) *wnt1* expression in controls (A,C,E) and *Zic1+4* morphants (B,D,F) at 16hpf (A,B), 19hpf (C,D) and 24hpf (E,F), lateral view (A-D) and dorsal view (E,F). *krox20* (red in A,B), provides a marker for r3 and r5. In hindbrain, *wnt1* is expressed in roof plate (RP) (black arrow in A) at elevated levels in rhombomere boundaries (white arrow in C) and in dorsal hindbrain regions (black arrowhead in E). We detected no change in *wnt1* expression in 16hpf *Zic1+4* morphants (B) compared to controls (A). By 19hpf elevated expression of *wnt1* in rhombomere boundaries (white arrow in C) is lost in *Zic1+4* morphants (white arrow in D indicates uniform expression in dorsal hindbrain). Reduced *wnt1* expression in rhombomere boundaries persists

at 24hpf in *Zic1+4* morphants (F, black arrowhead) compared to controls (E). Note that altered *wnt1* expression (F) is accompanied by a dorsal fused ventricle phenotype. (G-L) *rfng* expression in controls (G,I,K) and *Zic* morphants (H,J,L), lateral view (G-J) and dorsal view (K,L). Expression is not changed in 16hpf *Zic1+4* morphants (H) compared to controls (G). At 19hpf and 24hpf, down-regulation of *wnt1* expression in rhombomere boundaries in *Zic1+4* morphants is accompanied by expansion of *rfng*, expression into the rhombomere territory (J,L) compared to controls (I,K). No expansion is observed into r4 (J,L). (M-R) *zic1* expression in 18hpf and 24hpf controls (M,P), *Wnt1* morphants (N,Q) and *Rfng* morphants (O,R), dorsal view, and (V,Y) *zic4* expression in 24hpf controls (V), *Wnt1* morphants (W), and *Rfng* morphants (Y), dorsal view. The expression of *zic1* and *zic4* is not altered in the hindbrains of *Wnt1* morphants (N,Q,W) and *Rfng* morphants (O,R,Y) compared to controls (M,P,V). *Wnt1* knockdown (Q,W) and *Rfng* knockdown (R,Y) cause dorsal fused phenotypes similar to *Zic* and *Lmx* morphants.

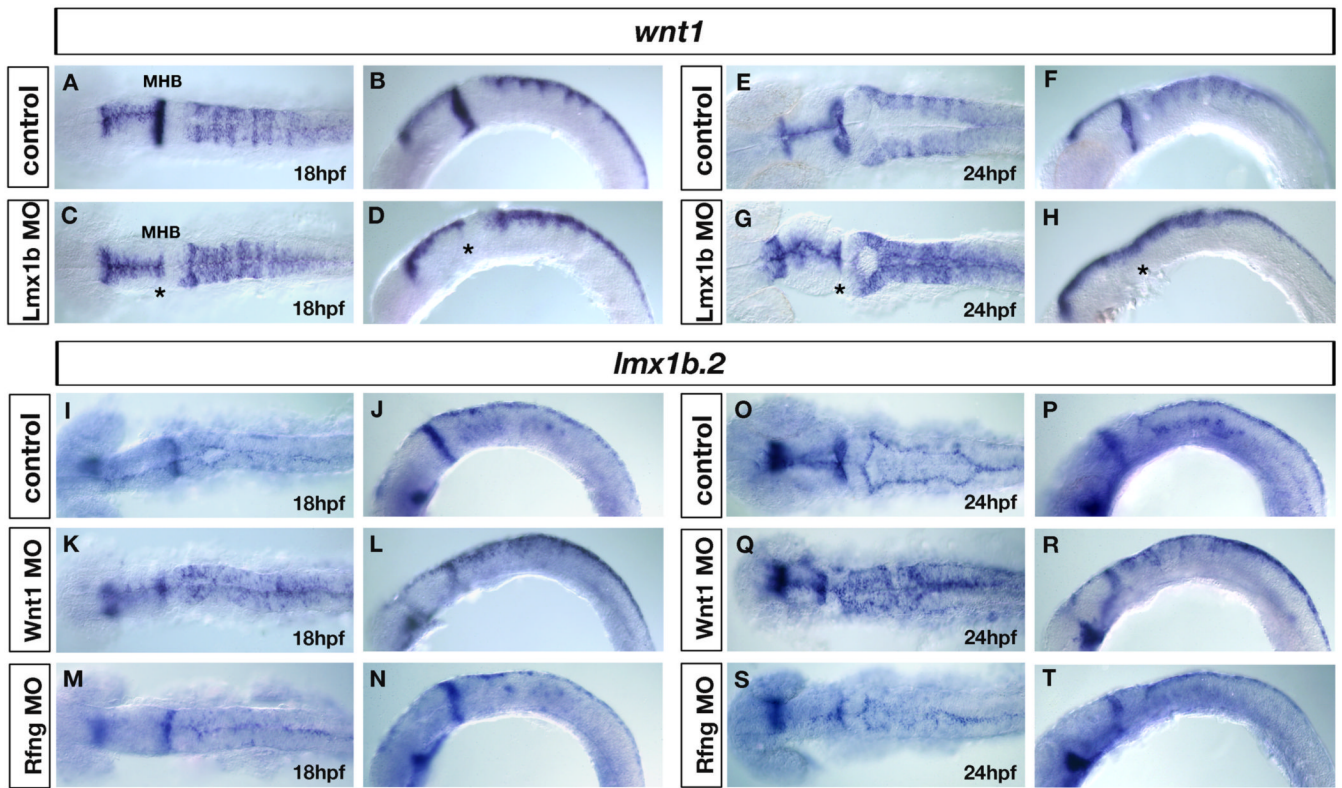


Fig. 7. Roof-plate dependent regulation of rhombomere boundary signals

(A-H) *wnt1* expression in controls (A,B and E,F) and *Lmx1b* double morphants (C,D and G,H) at 18hpf (A,B) and 24hpf (E,F), dorsal view (A,C and E,G) and lateral view (B,D and F,H). The *wnt1* expression pattern is not changed in *Lmx1b* morphants at 18hpf compared to controls (A-D), whereas in 24hpf *Lmx1b* morphants, *wnt1* expression is specifically down-regulated in rhombomere boundaries (F,H) compared to 24hpf controls (E,G). Notice the uniform expression of *wnt1* in the dorsal hindbrain of *Lmx* morphants (G,H), indicating that elevated levels of *wnt1* in rhombomere boundaries are not maintained in the absence of *lmx1b*-dependent roof plate development. Asterisks in C,D,G,H denote loss of *wnt1* expression in MHB (midbrain-hindbrain boundary) of *Lmx1b* morphants. (I-T) *lmx1b.2* expression in controls (I,J,O,P), *Wnt1* morphants (K,L,Q,R), and *Rfng* morphants (M,N,S,T) at 18hpf (I-N) and 24hpf (O-T), dorsal view (I,K,M,O,Q,S) and lateral view (J,L,N,P,R,T). In control embryos, dorsal hindbrain *lmx1b.2* expression is restricted to the roof plate cells (I,J,O,P), while in *Wnt1* morphants, *lmx1b.2* expression is expanded throughout the dorsal hindbrain (K, L,Q,R), indicating that dorsal hindbrain *Wnt1* signals are required for the restriction of *lmx1b.2* expression to the roof plate. By contrast, in *Rfng* morphants, in which *wnt1* signals are down-regulated exclusively in rhombomere boundaries (M,N,S,T), *lmx1b.2* expression is not altered compared to controls (I,J,O,P), indicating that rhombomere boundary-derived signals do not control the expression of *lmx1b.2* expression in the dorsal hindbrain.

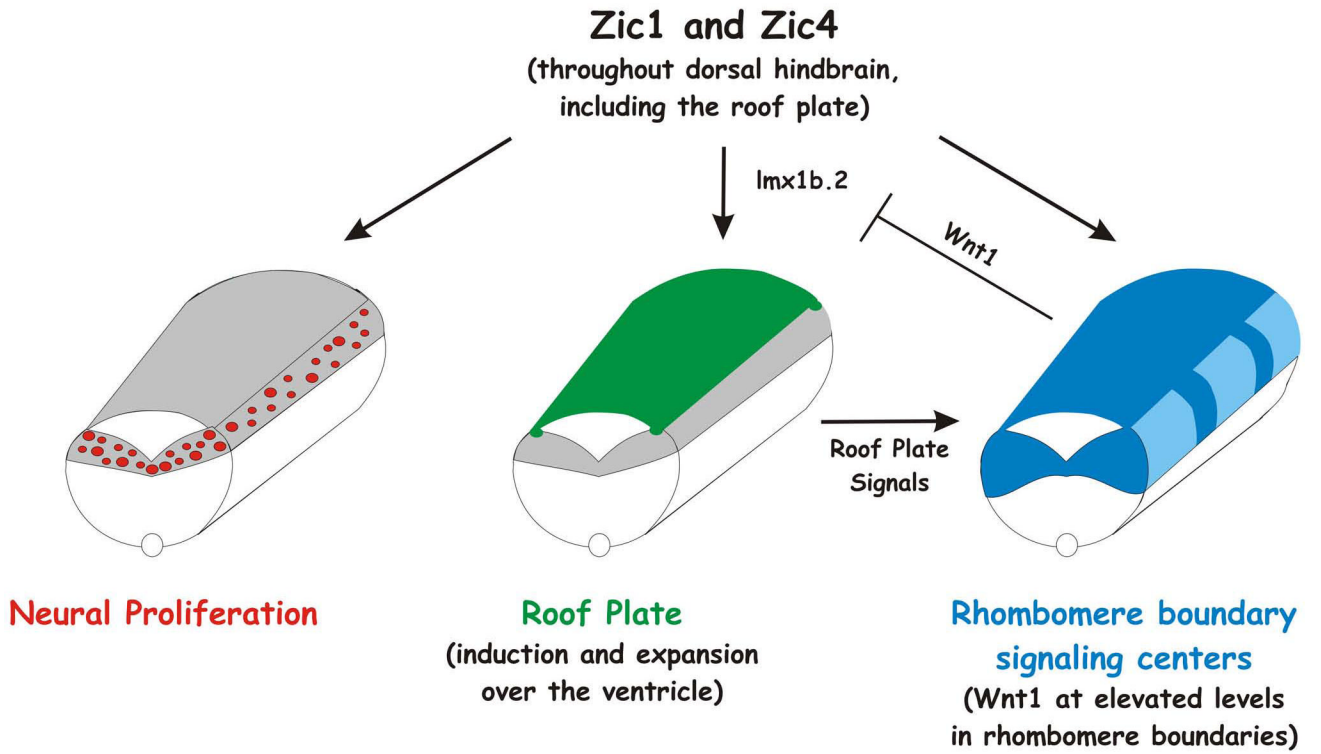


Fig. 8. Proposed model for the function of Zic1 and Zic4 in hindbrain development
Zic1 and Zic4 in the dorsal hindbrain regulate (1) neural proliferation (red), (2) dorsal roof plate specification (green), through genetic interaction with *lmx1b* genes, and (3) maintenance of dorsal rhombomere boundary signaling centers expressing *wnts* (dark blue). The outcome of these three developmental events is normal ventricle opening. Zics influence rhombomere boundary signaling centers in part via roof plate signals. Wnt1 in the roof plate (dark blue) and dorsal hindbrain (light blue) also functions independently of Zics to restrict *lmx1b* gene expression to the roof plate.

Concentration-dependent “dorsal fused” phenotype in *Zic* and /or *Lmx1b* morphants assessed at 24hpf in response to morpholinos targeted against 5'UTR (U) and/or ATG (A) of *zic1*, *zic4*, and *lmx1b.1*, *lmx1b.2* genes using a *zic1* as a dorsal molecular marker

Table 1

Condition	Total # of assessed embryos	No phenotype	Mild phenotype ⁱ	Intermediate phenotype ⁱⁱ	Severe phenotype ⁱⁱⁱ	% showing any phenotype
Control: IX Danieau buffer or unrelated MO	98	100%	---	---	---	0%
Zic1 MO (UTR+ATG)						
(U) 1mg/ml + (A) 1mg/ml =	87	70%	24%	4%	2%	30%
(U) 2mg/ml + (A) 2mg/ml =	81	13%	14%	25%	48%	87%
Zic4 MO (ATG)						
(A) 4mg/ml	74	80%	17%	3%	0%	20%
(A) 8mg/ml	94	9%	14%	16%	61%	91%
Zic1 MO (UTR+ATG) + Zic4 MO (ATG)						
Zic1(U) 1mg/ml + Zic1(A) 1mg/ml + Zic4(A) 4mg/ml	96	6%	7%	17%	70%	94%
Lmx1b.1 MO (ATG)						
(A) 2.5mg/ml	53	94%	6%	0%	0%	6%
(A) 5mg/ml	71	53%	38%	9%	0%	47%
Lmx1b.2 MO (ATG)						
(A) 2.5mg/ml	67	85%	14%	1%	0%	15%
(A) 5mg/ml	138	32%	11%	19%	38%	68%
Lmx1b.1 MO (ATG) + Lmx1b.2 MO (ATG)						
Lmx1b.1(A) 2.5mg/ml + Lmx1b.2(A) 2.5mg/ml	83	17%	13%	14%	56%	83%
Zic1 MO (UTR+ATG) + Lmx1b.2 MO (ATG)						
Zic1(U) 1mg/ml + Zic1(A) 1mg/ml + Lmx1b.2(A) 2.5mg/ml	61	8%	7%	11%	74%	92%
Zic4 MO (ATG) + Lmx1b.2 MO (ATG)						
Zic4(A) 4mg/ml + Lmx1b.2(A) 2.5mg/ml	52	6%	4%	10%	80%	94%

ⁱ **Mild phenotype:** one fusion along the dorsal hindbrain leading to incomplete ventricle morphogenesis or incomplete opening of the ventricle (Fig. 2F)

ⁱⁱ **Intermediate phenotype:** several fusions of the dorsal hindbrain leading to incomplete ventricle morphogenesis (Fig. 2E)

ⁱⁱⁱ **Severe phenotype:** complete fusion of the dorsal hindbrain up to rhombomere 1 leading to incomplete ventricle morphogenesis (Fig. 2D)